HHS Public Access

Author manuscript

Acta Neuropathol. Author manuscript; available in PMC 2023 July 28.

Published in final edited form as:

Acta Neuropathol. 2023 July ; 146(1): 97–119. doi:10.1007/s00401-023-02578-w.

Progranulin deficiency results in sex-dependent alterations in microglia in response to demyelination

Tingting Zhang[1], **Tuancheng Feng**[1], **Kenton Wu**[1], **Jennifer Guo**[1], **Alissa L. Nana**[2], **Guang Yang**[4], **William W. Seeley**[2,3], **Fenghua Hu**[1,#]

[1]Department of Molecular Biology and Genetics, Weill Institute for Cell and Molecular Biology, Cornell University, Ithaca, NY 14853, USA

[2]Department of Neurology, University of California, San Francisco, California 94158, USA.

[3]Department of Pathology, University of California, San Francisco, California 94158, USA.

[4]Department of Anesthesiology, Columbia University Irving Medical Center, New York, NY 10032, USA

Abstract

Heterozygous mutations in the *granulin* (*GRN*) gene, resulting in the haploinsufficiency of the progranulin (PGRN) protein, is a leading cause of frontotemporal lobar degeneration (FTLD). Complete loss of the PGRN protein causes neuronal ceroid lipofuscinosis (NCL), a lysosomal storage disorder. Polymorphisms in the *GRN* gene have also been associated with several other neurodegenerative diseases, including Alzheimer's disease (AD), and Parkinson's disease (PD). PGRN deficiency has been shown to cause myelination defects previously, but how PGRN regulates myelination is unknown. Here, we report that PGRN deficiency leads to a sex-dependent myelination defect with male mice showing more severe demyelination in response to cuprizone treatment. This is accompanied by exacerbated microglial proliferation and activation in the male PGRN deficient mice. Interestingly, both male and female PGRN-deficient mice show sustained microglial activation after cuprizone removal and a defect in re-myelination. Specific ablation of PGRN in microglia results in similar sex-dependent phenotypes, confirming a microglial function of PGRN. Lipid droplets accumulate in microglia specifically in male PGRN-deficient mice. RNA seq analysis and mitochondrial function assays reveal key differences in oxidative phosphorylation in male versus female microglia under PGRN deficiency. A significant decrease in myelination and accumulation of myelin debris and lipid droplets in microglia were found in the corpus callosum regions of FTLD patients with *GRN* mutations. Taken together, our data support that

[#]To whom correspondence should be addressed: Fenghua Hu, 345 Weill Hall, Ithaca, NY 14853, TEL: 607-2550667, FAX: 607-2555961, fh87@cornell.edu.

Author contributions

T.Z. performed most of the experiments and analyzed the data with the help of K.W. and J. G. T. F. helped with western blot and immunostaining analysis. G.Y provided and helped with *Cx3cr1*$^{+/CreER}$, *Grn* $^{flox/flox}$ mouse genotyping. A.N.L. provided human patient samples under the guidance of W.W.S. F.H. supervised the project and wrote the manuscript with T.Z. All authors read and approved the final manuscript.

Conflict of interest

The authors declare that they have no conflict of interest.

Ethical Approval and Consent to Participate

All applicable international, national, and/or institutional guidelines for the care and use of animals were followed. The work under animal protocol 2017–0056 is approved by the Institutional Animal Care and Use Committee at Cornell University.

PGRN deficiency leads to sex-dependent alterations in microglia with subsequent myelination defects.

Keywords

Progranulin (PGRN); myelination; microglia; sex; frontotemporal lobar degeneration (FTLD)

Introduction

Frontotemporal lobar degeneration (FTLD) is a common cause of dementia in people under the age of 60 [15]. Haploinsufficiency of progranulin (PGRN), due to heterozygous mutations in the *GRN* gene, is one of the major genetic causes of FTLD with aggregates containing TAR DNA binding protein 43 (TDP-43) [5,13,22]. *GRN* mutations have been identified in 20–25% of familial FTLD cases and about 10% of all FTLD cases, and these mutations have been shown to reduce PGRN levels or result in loss of PGRN function [48].

Interestingly, complete loss of PGRN in humans causes neuronal ceroid lipofuscinosis (NCL) [2,70], a lysosomal storage disease. In addition, PGRN polymorphisms contribute to developing the risk of Alzheimer's disease (AD)[41,45,58,66,86], with serum PGRN levels inversely proportional to the risk of AD development [36]. *GRN* has also been identified as one of the main risk factors for limbic-predominant age-related TDP-43 encephalopathy (LATE)[54]. Furthermore, a recent study identified *GRN* as one of the two main determinants of differential aging in the cerebral cortex with genome-wide significance[61]. Thus, PGRN is intimately linked to brain aging and neurodegeneration.

PGRN is an evolutionarily conserved glycoprotein of 88 kDa comprised of 7.5 granulin repeats (para-granulin and granulins A, B, C, D, E, F, G) [6,55]. In the brain, PGRN is mainly expressed in neurons and microglia and has been reported to possess various neuroprotective functions and play a key role in microglia-mediated inflammation [42,51,75,77]. Microglia are the resident immune cells in the central nervous system (CNS) and maintain CNS homeostasis through the clearance of apoptotic bodies and debris, synaptic pruning, and secretion of neurotrophic factors[1,12,26,29,31]. Misregulation of microglia-mediated inflammation is a common mechanism shared by many neurodegenerative diseases[1,12,26,29,31].

Myelination, the formation of the lipid-rich myelin sheath around axons, is essential not only for action potential propagation but also for axon maintenance and is intimately linked to brain health [63]. Recently, FTLD- *GRN* mutation individuals have been shown to develop multifocal myelin loss [10,84] and microglial accumulation of myelin debris in the white matter of the brain [85]. Myelination defects have also been reported in aged PGRN-deficient mice [38,74] In addition, variability in the *GRN* gene has been shown to increase the risk for primary progressive multiple sclerosis (MS), an autoimmune myelination disorder, specifically in males [20]. PGRN expression is upregulated in microglia in MS patients [83] and *GRN* polymorphisms influence disease course and relapse recovery in MS [82]. However, underlying mechanisms remain unclear. In this study, we investigated the role of PGRN in myelination using the cuprizone-induced demyelination model. We

found that PGRN regulates the myelination process by modulating microglial activities in a sex-dependent manner.

Material and Methods

Mouse strains and treatment

Wild type C57/BL6, *Cx3cr1*$^{+/CreER}$ [56], *Grn* $^{flox/flox,}$ and *Grn*$^{-/-}$ mice [88] were obtained from the Jackson Laboratory. *Cx3cr1*$^{+/CreER}$ *Grn* $^{flox/flox}$ mice were fed tamoxifen at 3 weeks of age to delete PGRN in microglia[56]. *Cx3cr1*$^{+/CreER}$ mice were also fed tamoxifen to be used as controls. Tamoxifen (Sigma T5648, 10mg/ml) was dissolved in filter-sterilized corn oil by incubating overnight at 37°C. The solution was protected from light and was administered to mice (75 mg /kg) via oral gavage every other day 7 times total. CNS demyelination was induced by supplementing the diet of 10-week-old mice with 0.2% (w/w) cuprizone (bis [cyclohexanone] oxaldihydrazone) in powdered rodent chow [72]). The rodent chow (5 g/mouse/day) was replaced every other day for 5 weeks. For the remyelination period, mice were returned to normal chow for 3 weeks. Untreated control mice were fed normal crushed chow for 5 weeks or 8 weeks. All the mice were housed in the Weill Hall animal facility at Cornell. All animal procedures have been approved by the Institutional Animal Care and Use Committee (IACUC) at Cornell.

Antibodies and Reagents

The following antibodies were used in this study: mouse anti-Galectin-3 (BioLegend, 126702), goat anti-human GPNMB (R&D Systems, AF2550), goat anti-mouse GPNMB (R&D Systems, AF2330), rat anti-mouse LAMP1 (BD Biosciences, 553792), rabbit anti-IBA-1 (Wako, 01919741), goat anti-AIF-1/Iba1 (Novus Biologicals, NB100–1028), rat anti-CD68 (Bio-Rad, MCA1957), and sheep anti-PGRN (R&D Systems, AF2557), mouse anti-MBP (Millipore, SMI-99), Goat anti-Olig2 (R&D Systems, AF2418), mouse anti-APC (Millipore, OP80), rabbit anti-Perilipin2 (Proteintech Group,15294-1-AP), sheep anti-TREM2 (R&D Systems, AF1729). Detailed information is provided in Supplementary Table 1.

The following reagents were also used in the study: Dulbecco's modified Eagle's medium (DMEM)(Cellgro, 10–017-CV), Hanks' Balanced Salt Solution (HBSS) (Cellgro, 21–020-CV), Dulbecco's modified Eagle's medium/Ham's F-12 (DMEM/F-12)(Cellgro, 10–092-CV), 0.25% Trypsin (Corning, 25–053-CI), Autofluorescence Quencher (Biotium, 23007), Odyssey blocking buffer (LI-COR Biosciences, 927–40000), and O.C.T compound (Electron Microscopy Sciences, 62550–01).

Primary microglia cell culture

Microglia were isolated from postnatal day 0–2 female and male pups according to a published protocol [94]. Briefly, cortices were rapidly dissected from the brain in 2ml cold HBSS at 4°C followed by digestion with 0.25% trypsin. The cells were maintained in DMEM/F12 with 10% FBS at 37 °C in a 5% CO_2-humidified atmosphere. GM-CSF (R&D system) was added at 5 ng/ml to stimulate microglial proliferation. The flasks were shaken to separate microglia from mixed glial cultures after 14 days in culture. The purity of

primary microglia was greater than 95% validated by IBA1 immunostaining. After 24 hours, the cultured medium was replaced with a fresh medium used for experiments.

Oxygen consumption rate (OCR) measurement

The oxygen consumption rate (OCR) of primary microglia was measured using a Seahorse XF Cell Mito Stress Test Kit (103015–100, Agilent Technologies) with a Seahorse XFe 96 Extracellular Flux Analyzer (Seahorse Bioscience) according to the manufacturer's instructions [65]. Briefly, triplicates or quadruplicates of microglia were plated on XF-96 cell culture microplates overnight and then treated with or without purified myelin (10ug/ml) for 24 hours. Microglia were washed and analyzed in the XF assay medium (10 mM glucose, 1 mM pyruvate sodium, 2 mM L-Glutamine). Measurements were obtained in real-time with no drug treatment (basal conditions) and with the sequential treatment of 1 μM oligomycin, 2 μM FCCP, and 0.5 μM rotenone plus antimycin A (Rote/AA). After the measurements, the number of cells within the plate was determined by Hoechst staining and subsequent counting of nuclei. Data were analyzed using Seahorse XF 96 Wave software and the results were represented as pmol/min, and then normalized by the cell number. OCR measurement under basal conditions in the absence of drugs represents the basal OCR. Spare respiratory capacity was calculated as the differences between the basal OCR and the maximal OCR after FCCP addition. Experiments were repeated three times with different batches of male and female WT and *Grn*$^{-/-}$ microglia cultured independently.

Brain tissue

Human brain tissues were obtained from the Neurodegenerative Disease Brain Bank at the University of California, San Francisco. Authorization for autopsy was provided by the patients' next-of-kin, and procedures were approved by the UCSF Committee on Human Research. Neuropathological diagnoses were made in accordance with consensus diagnostic criteria [39,49]. Cases were selected based on neuropathological diagnosis and genetic analysis. Formalin-fixed, paraffin-embedded tissue sections of the corpus callosum were used from subjects with FTLD-TDP type A with *GRN* mutations and healthy controls. Healthy control tissues were obtained from individuals without dementia who had minimal age-related neurodegenerative changes. Detailed information is provided in Table 1.

Immunohistology and analysis

For paraffin-embedded human brain samples, 8 um-thick sections including the corpus callosum were deparaffinized with xylene and ethanol. Antigen retrieval was performed by microwaving in citrate buffer (pH 6.0) for 20 min. For mouse brain immunostaining, mice were anesthetized with isoflurane transcardially perfused with PBS and 4% paraformaldehyde (PFA). The brains were removed and continuously postfixed overnight in 4% PFA at 4°C. After being dehydrated, coronal brain sections including cortex and corpus callosum (overlying the fornix approximately between bregma 0.86 and 0.14 mm) were cut using a cryostat (Leica, Heidelberg, Germany) and processed for immunostaining.

Sections were first permeabilized and blocked with 0.1% saponin in Odyssey blocking buffer and incubated with primary antibodies overnight at 4°C. Sections were washed with PBS three times followed by incubation with secondary fluorescent antibodies and Hoechst

at room temperature for two hours the next day. Images were acquired on a CSU-X spinning disc confocal microscope (Intelligent Imaging Innovations) with an HQ2 CCD camera (Photometrics) using 63X and 100X objectives or on a Leica DMi8 inverted microscope with a 20X objective. Three to five non-adjacent brain sections per mouse were used. Ten to fifteen different random confocal images were captured from the corpus callosum region of mouse brain sections. Five to ten random fields of the corpus callosum were examined for human brain sections.

For the quantitative analysis of MBP and IBA1 levels in the mouse or human brain sections, the fluorescence intensity was measured directly using ImageJ software (National Institutes of Health, Bethesda, MD, USA) after a threshold application. The protein levels were determined by the total fluorescence signals. For the quantitative analysis of CD68, Galectin3, GPNMB, and TREM2 levels in microglia, the IBA1+ microglia were selected using the region of interest (ROI) tool after the data channels were separated (Image\Color\Split Channels). Next, CD68, Galectin3, GPNMB, and TREM2 signals within the IBA1 ROI were selected (Analyze\tools\ROI manager) and measured.

The number of IBA1+ microglia, perilipin2+IBA1+ microglia, Olig2+ cells (representing all oligodendrocyte lineage cells), and APC-positive cells (APC+, mature oligodendrocyte cells) was counted using the “analyze particles” function of ImageJ after a threshold application. Perilipin2 positive area in microglia was quantified using ImageJ after a threshold application.

Microglia morphometric analysis was performed using ramification index (RI) ($4\pi \times$ cell area/(cell perimeter)^2) as previously described [9,30]. Cell area and perimeter were calculated with Image J. 10–15 microglia were analyzed for mice fed with a normal diet. A total of 60 to 70 cells were analyzed from 3 to 5 independent mice for each cuprizone treated and recovery group.

RNA-seq analysis

CD11b+ microglia were isolated from adult mouse brains using Magnetic-activated cell sorting (MACS) according to published protocols [32,44]. The purity of microglia was verified by immunoblotting with microglia marker IBA1, astrocyte marker GFAP, and neuronal marker NeuN. Total RNA was extracted from isolated microglia using Trizol (Thermo scientific). RNA quality was checked using nanodrop, gel electrophoresis, and Agilent Fragment Analyzer. RNAseq libraries were generated by the Cornell TREx Facility using the NEBNext Ultra II Directional RNA Library Prep Kit (New England Biolabs) using 700ng input total RNA per sample. At least 20M reads (2×150nt PE) were generated on a NovaSeq (Illumina). Reads were trimmed to remove low-quality and adaptor sequences with TrimGalore (a wrapper for cutadapt and fastQC), requiring a minimum trimmed length of 50nt. Reads that passed quality control were aligned to reference genome (mouse GRCm38/mm10) [89] using STAR [17], using ‘--quantMode GeneCounts’ to output counts per gene. SARTools [80] and DESeq2 [46] were used to generate normalized counts and statistical analysis of differential gene expression. Genes with FDR control p-value ≤ 0.05 and log fold change ≥ 0.5 were identified as differentially expressed genes (DEGs). Heatmap of the DEGs was generated by using Heatmapper [4]. Enrichment analysis using Hallmark gene

sets and Kyoto Encyclopedia of Genes and Genomes (KEGG) pathway analyses (KEGG) gene sets was performed using Gene Set Enrichment Analysis (GSEA)[73]. GSEA was applied using the list of all genes expressed, ranked by the fold change with recommended default settings (1,000 permutations and a classic scoring scheme). The false discovery rate (FDR) was estimated to control the false-positive finding of a given normalized enrichment score (NES) by comparing the tails of the observed and null distributions derived from 1,000 gene set permutations. The gene sets with an FDR of <0.05 were considered significantly enriched.

Statistical analysis

In all experiments, data were expressed as mean ± standard error of the mean (SEM). Statistical significance was assessed by unpaired Student's t-test (for two groups comparison) or Two-way ANOVA tests with Bonferroni's multiple comparisons (for multiple comparisons). All statistical analyses were performed using GraphPad Prism software (GraphPad Software, San Diego, CA). P values less than or equal to 0.05 were considered statistically significant. *p < 0.05; **p < 0.01; ***p < 0.001; ****p < 0.0001.

Results

Male *Grn*$^{-/-}$ mice are more susceptible to cuprizone-induced demyelination and fail to re-myelinate

To investigate the role of PGRN in myelination, we treated wild-type (WT) and *Grn*$^{-/-}$ mice with cuprizone (CPZ) for 5 weeks to induce the apoptosis of mature oligodendrocytes and demyelination [25,52,95]. Mice were then fed with a normal diet for 3 weeks to allow recovery and remyelination (Fig. 1a). After 5 weeks of treatment, cuprizone-induced demyelination was observed in multiple regions of WT and *Grn*$^{-/-}$ mice based on immunostaining of myelin basic protein (MBP), including the cortex and the corpus callosum (CC), as previously reported for cuprizone [52,69] (Fig. 1b–1e). Interestingly, PGRN loss leads to exacerbated myelin loss in the male but not female mice after 5 weeks of cuprizone treatment compared to age and sex-matched WT control (Fig.1b-1e), supporting a sex-dependent effect of PGRN on demyelination in response to cuprizone treatment. After 3 weeks of cuprizone removal and recovery, MBP intensities were restored close to the normal levels in the WT mice (Fig. 1b–1e), indicating successful remyelination. However, the reduction of MBP levels persists in both male and female PGRN-deficient mice (Fig. 1b–1e). Taken together, our data support that PGRN deficiency leads to exacerbated demyelination in males but not in females in response to cuprizone and a failure to re-myelinate in both male and female mice after cuprizone removal.

To determine changes in oligodendrocytes during demyelination and remyelination, we examined the numbers of total and mature oligodendrocytes at different time points using Olig2 and APC as markers, respectively. Although both WT and *Grn*$^{-/-}$ mice showed a decrease in the number of total (Olig2^{+}) and mature (APC^{+}Olig2^{+}) oligodendrocytes following 5 weeks of cuprizone treatment, the reduction in the number of mature but not total oligodendrocytes is significantly more pronounced in the male *Grn*$^{-/-}$ mice compared with WT mice (Fig. 2a–2c), supporting increased death of mature oligodendrocytes in male

Grn$^{-/-}$ mice upon cuprizone treatment. In addition, three weeks after cuprizone removal, the number of mature oligodendrocytes returned to normal conditions in WT mice. However, a decreased number of mature oligodendrocytes and a decreased ratio in the number of mature oligodendrocytes (APC+Olig2+) to the number of total oligodendrocytes (Olig2+) were observed in male *Grn*$^{-/-}$ mice compared with WT mice (Fig. 2d), indicating impaired differentiation of oligodendrocyte precursor cells (OPCs) in male *Grn*$^{-/-}$ mice during recovery. However, oligodendrocyte differentiation defects during the recovery were not observed in the female *Grn*$^{-/-}$ mice (Fig. 2d), further supporting a sex-dependent effect of PGRN on myelination. The fact that female mice also show myelination defects as shown by decreased MBP intensity (Fig. 1e) supports that the myelination process but not oligodendrocyte differentiation is affected by PGRN loss in females.

PGRN deficiency leads to more pronounced microglial activation in male mice in response to demyelination

Cuprizone-induced death of oligodendrocytes is known to result in the accumulation of myelin debris and activation of microglia [95]. Since PGRN is known to play a critical role in microglial activation [42], we examined PGRN expression in microglia in response to cuprizone treatment. An obvious increase in PGRN levels was found in IBA1-positive microglia in the corpus callosum region after 5 weeks of cuprizone treatment as we previously reported [90] (Fig. 3a). Next, we examined whether microglial proliferation and activation in response to cuprizone are altered by PGRN deficiency by analyzing microglia number and microglia morphology. A significant increase in the number of IBA1 positive (IBA1+) microglia was observed in the male but not female *Grn*$^{-/-}$ mice compared to sex-matched WT controls after 5 weeks of cuprizone treatment (Fig. 3b–3c). In addition, 3 weeks after cuprizone removal, the number of IBA1+ microglia in WT mice is greatly reduced (Fig. 3b–3c). However, this decrease is not observed in either male or female *Grn*$^{-/-}$ mice after cuprizone removal (Fig. 3b–3c).

To determine changes in microglial morphology, we used a ramification index according to previous studies [9,30]. The microglia in a resting state display a ramified morphology with a ramification index (RI) value close to zero and acquire an amoeboid shape once activated with a ramification index (RI) value close to one. Five weeks after CPZ treatment, *Grn*−/− microglia acquire a typical activated amoeboid shape in both male and female mice (Fig. 3d). The RI for *Grn*−/− microglia is significantly higher than the RI of WT microglia in both male and female mice, with a bigger difference between WT and *Grn*−/− in male mice (Fig. 3d). Three weeks after cuprizone removal, WT microglia return to a ramified shape with the RI significantly lower compared to that of 5 weeks after CPZ treatment. However, *Grn*−/− microglia in both male and female mice remain amoeboid shape with a RI significantly higher than WT microglia 3 weeks after cuprizone removal (Fig. 3d), indicating prolonged microglial activation and a failure of microglia to return to normal homeostasis in PGRN deficient mice after demyelination.

Next, we determined whether microglial activation status in response to demyelination is altered by PGRN deficiency. We examined the protein levels of TREM2, Galectin3, GPNMB, and CD68, markers for disease-associated microglia (DAM), which are known

to get upregulated in microglia in response to demyelination and other disease conditions [35,59]. After 5 weeks of cuprizone treatment, male but not female *Grn*$^{-/-}$ mice showed significantly increased protein levels of CD68, Galectin3, and TREM2 in microglia compared to sex-matched WT controls (Fig. 4a–b and Fig. 5a–d), indicating that PGRN deficiency leads to enhanced microglial activation in response to demyelination in male but not female mice. Interestingly, the levels of another DAM marker, GPNMB, which was recently identified as the most up-regulated protein in response to PGRN loss [18,38], are elevated in microglia in both male and female *Grn*$^{-/-}$ mice compared to sex-matched WT controls after 5 weeks of cuprizone treatment (Fig. 5c, 5d). Thus, PGRN deficiency only affects the expression of a subset of DAM markers in a sex-dependent manner.

Three weeks after cuprizone removal, microglial expression of TREM2, Galectin3, GPNMB, and CD68 returns to normal levels in WT mice (Fig. 4 and Fig. 5). However, the levels of these proteins remain elevated in microglia in both male and female *Grn*$^{-/-}$ mice. This result is consistent with our IBA1 staining results and supports an important sex-independent role of PGRN in the resolution of microglial activation in response to demyelination.

Microglial accumulation of lipid droplet and lipofuscin in PGRN deficient mice

Recently PGRN deficient microglia have been shown to accumulate lipid droplets upon aging [50]. Lipid droplet-associated microglia are commonly found during neurodegeneration and are thought to represent a dysfunctional and pro-inflammatory state with altered metabolism [11,50]. To determine whether lipid storage is affected by PGRN loss in response to demyelination, we stained brain sections from WT and *Grn*$^{-/-}$ mice with antibodies against microglial marker IBA1 and perilipin 2, a protein associated with lipid droplets. We found a dramatic increase in the number of microglia with perilipin 2 positive puncta in the male *Grn*$^{-/-}$ mice with cuprizone treatment (Fig. 6a–6b). A further increase was detected 3 weeks after cuprizone removal. This increase in lipid droplet accumulation is not observed in female *Grn*$^{-/-}$ mice compared to age and sex-matched WT control both in the cuprizone-treated and recovery group (Fig. 6a–6b). Thus, the loss of PGRN leads to a significant defect in lipid metabolism in male mice but not in female mice in response to cuprizone-induced demyelination.

In addition, the accumulation of lysosomal substrates in microglia has been shown to result in autofluorescence and impaired functions during aging [8]. We observed a significant accumulation of the autofluorescent material lipofuscin in microglia in the male but not female *Grn*$^{-/-}$ mice (Fig. 6c, 6d), which could be caused by lipid overloading in the male *Grn*$^{-/-}$ mice.

Microglia-specific ablation of PGRN results in myelination defects and exacerbated microglia activation in male mice but not female mice

The exacerbated demyelination in response to cuprizone and failed re-myelination in PGRN-deficient mice could be caused by PGRN loss in neurons, oligodendrocytes, or microglia. To further confirm the role of microglia in inducing myelination defects in PGRN-deficient mice, we specifically deleted PGRN in microglia by expressing the tamoxifen-

inducible Cre recombinase under the control of the CX3CR1 promoter (*Cx3cr1*$^{+/CreER}$) [56]. *Cx3cr1*$^{+/CreER}$ *Grn* $^{flox/flox}$ mice were fed with tamoxifen to activate Cre-mediated recombination specifically in microglia. *Cx3cr1*$^{+/CreER}$ mice were used as controls. These mice were then treated with cuprizone for 5 weeks, or treated with cuprizone for 5 weeks and then allowed to recover for 3 weeks before tissue collection (Fig. 7a). The ablation of PGRN was confirmed by immunostaining (Fig. 7b). Brain sections were also stained with anti-MBP antibodies to determine alterations in myelination. Consistent with the data from whole-body knockout, microglia-specific ablation of PGRN leads to exacerbated demyelination in response to cuprizone in male mice and a defect in re-myelination in both male and female mice (Fig. 7c–7d), supporting that PGRN functions in microglia to regulate the myelination process.

Furthermore, PGRN deficiency in microglia results in enhanced microglial proliferation and activation as shown by an increased number of IBA1+ microglia (Fig. 7e, 7f), amoeboid like morphology (Fig. 7g) and elevated levels of IBA1 and CD68 (Supplementary Fig. 1a, 1b) in the male but not female mice 5 weeks after cuprizone treatment. In contrast to whole-body PGRN deficiency (Fig. 4b), CD68 and IBA1 levels and the number of IBA1+ microglia are comparable in female *Cx3cr1*$^{+/CreER}$ and *Cx3cr1*$^{+/CreER}$ *Grn* $^{flox/flox}$ mice three weeks after cuprizone removal (Fig. 7e, 7f; Supplementary Fig. 1a, 1b,). Intriguingly, we failed to see a decrease in the number of IBA1+ microglia or a return of microglia morphology to the ramified state 3 weeks after cuprizone removal in both *Cx3cr1*$^{+/CreER}$ and *Cx3cr1*$^{+/CreER}$ *Grn* $^{flox/flox}$ mice (Fig. 7e–7g), suggesting that haploinsufficiency of CX3CR1 might lead to a defect in microglia deactivation during the recovery phase.

The lack of differences in microglial recovery between female *Cx3cr1*$^{+/CreER}$ and *Cx3cr1*$^{+/CreER}$ *Grn* $^{flox/flox}$ is unexpected considering the strong phenotypes observed in whole-body female PGRN deficient mice (Fig. 4 and 5) and known lysosomal functions of PGRN. While it might suggest a potential function of PGRN in other cell types that help deactivate microglia in the female whole body *Grn*$^{-/-}$ mice during recovery, an alternative explanation is that haploinsufficiency of CX3CR1 causes alterations in microglia that have masked the difference caused by PGRN deficiency. Since GPNMB is the strongest marker associated with PGRN deficiency[18,38], next we examined GPNMB expression levels in *Cx3cr1*$^{+/CreER}$ and *Cx3cr1*$^{+/CreER}$ *Grn* $^{flox/flox}$ mice in response to cuprizone treatment. Interestingly, PGRN deficiency in microglia leads to significantly increased levels of GPNMB in both male and female mice in response to cuprizone treatment and during the recovery phase (Supplementary Fig. 1c–d). Since increased levels of GPNMB reflect lysosomal dysfunction [79], these data support that PGRN deficiency in microglia leads to lysosomal dysfunction in a sex-independent manner.

PGRN deficiency leads to sex-dependent alterations in oxidative phosphorylation in microglia

To further dissect the function of PGRN in microglia, we isolated microglia from WT and *Grn*$^{-/-}$ mice with or without cuprizone treatment using magnetic beads coated with antibodies against CD11b, a cell surface transmembrane protein commonly used as a marker for microglia [40]. The gene expression profiles in these microglia were analyzed

by bulk RNA seq (Supplementary Dataset 1). Interestingly, the oxidative phosphorylation pathway shows opposite regulation in male versus female microglia under PGRN deficiency with a decrease in expression in male microglia but an increase in expression in female microglia after 5 weeks of cuprizone treatment based on Gene Set Enrichment Analysis (GSEA) (Supplementary Fig. 2a–d). Since decreased oxidative phosphorylation could result in increased accumulation of lipid droplets[11], which we have observed in the male PGRN deficient microglia, we analyzed possible changes in oxidative phosphorylation in cultured primary microglia using the Seahorse mitochondrial stress test kit. Consistent with our RNA seq analysis, we found PGRN deficiency leads to a significant decrease in the maximum and spare respiration capacity as shown by oxygen consumption rate (OCR) specifically in male microglia in response to myelin treatment (Fig. 8a, 8b). A decrease in the basal respiration rate and the ATP-linked respiration was also observed in male *Grn*$^{-/-}$ microglia compared to sex-matched WT controls but did not reach statistical significance (Fig. 8a). No difference in OCR was observed in female *Grn*$^{-/-}$ microglia (Fig. 8b). Taken together, our results support a loss of mitochondria function specifically in the male PGRN deficient microglia in response to myelin challenge, which could lead to alterations in lipid metabolism and microglial activation states.

Myelin loss and microglia activation in the white matter of FTLD-*GRN* patients

To investigate the role of PGRN in myelination in humans, we examined myelination defects in the postmortem brain samples of patients with FTLD-TDP and carrying a *GRN* mutation (FTLD-GRN) (Table 1). Sections from the corpus callosum regions were stained with antibodies against MBP and IBA1. To determine any gender-specific effect of PGRN haploinsufficiency on myelination, we analyzed male and female patient samples separately. Additionally, since the FTLD risk factor TMEM106B is known to play a role in myelination [19,92], we also considered *TMEM106B* genotypes in our analysis. It has been shown that *TMEM106B* allele rs1990622^{A} acts as a risk factor and rs1990622^{G} reduces the odds of patients with *GRN* mutations developing FTLD[78]. Due to the limited sample size, we only examined samples with *TMEM106B* rs1990622$^{A/G}$ and rs1990622$^{G/G}$ genotypes. A significant reduction in MBP staining intensity was found in male patients with FTLD-*GRN* compared to control subjects (Fig. 9a–9b). No significant difference was found in females, although there is a trend of reduction, probably due to low sample size and large variability among the samples since we only have four samples from female patients with FTLD-*GRN* with either *TMEM106B* rs1990622$^{A/G}$ or *TMEM106B* rs1990622$^{G/G}$ genotypes. A significant increase in IBA1 and GPNMB staining intensities and the number of IBA1-positive microglia was observed in both male and female patients with FTLD-*GRN* compared to control subjects (Fig. 9a, 9c, 9d). In addition, a decrease in the intensity of myelin basic protein is observed in both male and female FTLD-*GRN* patients compared to control subjects, but only reaching significance in the males and when female and male samples were combined (Fig. 9b). In addition, myelin accumulation in the IBA1 positive microglia is frequently observed in samples from both male and female patients with FTLD-*GRN* (Fig. 9a), consistent with the results from a recently published study [85]. Moreover, a significant increase in the percentage of lipid droplet-containing microglia was observed in the corpus callosum regions in the FTLD-*GRN* patient samples (Supplementary Fig. 3). Due to low sample size, it is difficult to determine whether there is a gender-dependent effect

of PGRN loss. Nevertheless, this indicates a failure of microglia in clearing myelin debris and a defect in microglial lipid metabolism due to PGRN deficiency. It should be noted that heterozygous mutations in the *GRN* gene, resulting in PGRN haploinsufficiency, lead to FTLD in humans [5,13,22]. However, PGRN haploinsufficiency in mice does not have any obvious phenotypes [62] and thus homozygous PGRN knockout mice were used in our study.

Discussion

PGRN regulates microglial activities to modulate the myelination process

In response to demyelination, microglia help remove myelin debris, recycle lipids and promote the differentiation of oligodendrocyte precursor cells and subsequent remyelination [53,60,64,68]. The critical roles of microglia in myelination are supported by the results of our study. PGRN expression levels are increased in microglia in response to demyelination (Fig. 3a). In male mice, specific ablation of PGRN in microglia recapitulates the myelination defects seen in whole-body PGRN knockout mice, including exacerbated demyelination in response to cuprizone treatment and failed remyelination upon cuprizone removal (Fig. 7c,7d). In female mice, PGRN deficiency in microglia also results in a myelination defect during recovery (Fig. 7c,7d). In addition, myelin debris accumulates in microglia under PGRN-deficient conditions in FTLD-*GRN* patients (Fig. 9) [85].

PGRN is also expressed in other cell types, including neurons, oligodendrocytes, and astrocytes. PGRN is known to promote neuronal survival and axon outgrowth [7,21,23,77], thus PGRN deficiency might interfere with neuronal recovery after demyelination. Increased astrogliosis has also been reported under PGRN deficiency [42]. In addition, PGRN expression can be detected in oligodendrocytes at the protein level (data not shown), although the function of PGRN in oligodendrocytes remains to be explored. Thus, PGRN deficiency is likely to result in slower recovery of neurons, astrocytes, and oligodendrocytes to the normal homeostasis after cuprizone withdrawal, which might contribute to the prolonged microglial activation and myelination defects seen in whole-body PGRN knockout mice. Nevertheless, our results from microglia-specific ablation of PGRN strongly support the critical role of PGRN in microglia regulating the myelination process.

Sex-dependent alterations in microglial dynamics in PGRN deficient mice in response to demyelination

In this study, we demonstrated sex-dependent alterations in microglial dynamics in PGRN deficient mice in response to demyelination: (1) Male but not female PGRN knockout mice show exacerbated demyelination in response to cuprizone treatment (Fig. 1&2); (2) Male but not female PGRN knockout mice show increased microglial proliferation and activation after 5 weeks of cuprizone treatment (Fig. 3–5); (3) Male but not female PGRN deficient microglia show significantly increased lipid droplet accumulation and lipofuscin accumulation after cuprizone treatment (Fig.6); (4) Microglia specific deletion of PGRN causes more severe myelination defects in males but not in females in response to cuprizone treatment (Fig. 7); (5) In cell culture, male but not female $Grn^{-/-}$ microglia show significantly decreased mitochondrial functions in response to myelin treatment (Fig. 8); (6)

In the postmortem FTLD-*GRN* human patient samples, *GRN* mutations result in a decreased myelination in both male and females, but the effect is only significant in males with the limited samples we have. All these data show key differences in microglial dynamics in male versus female $Grn^{-/-}$ microglia in response to demyelination. Our results might also explain the finding that *GRN* gene variability is significantly linked to the risk for MS in males but not in females [20].

The molecular basis for the observed sex dimorphism remains to be fully explored. Many differences have been reported between males and females in their innate and adaptive immune responses [43]. Microglial functionality is also known to differ between males and females during development, aging, and under disease conditions, such as stroke, and experimental autoimmune encephalomyelitis (EAE) [76] [27,28,47]. A recent study has demonstrated sex-dependent dysregulation in the periphery and central immune system as a result of PGRN deficiency [34]. Our RNA seq analysis (Supplementary Fig. 2) suggested that the activity of oxidative phosphorylation might be regulated differently upon PGRN loss in male and female microglia in response to cuprizone-induced demyelination. We confirmed this with the mitochondrial stress test, which showed that male $Grn^{-/-}$ microglia has significantly reduced maximum respiration and spared respiration capacity in response to myelin treatment compared to WT control (Fig. 8). Since oxidative phosphorylation is directly linked to lipid metabolism[11], decreased respiration capacity could lead to increased lipid accumulation and lipid droplet formation and likely alter the microglial activation state in male $Grn^{-/-}$ microglia (Fig. 10). Mitochondrial dysfunction could also contribute to lysosomal abnormalities, resulting in a specific accumulation of lipofuscin in the male $Grn^{-/-}$ microglia (Fig. 6c, 6d), due to poor lysosomal acidification by the V-ATPase proton pump with low ATP supply from the mitochondria [71].

Regulation of mitochondrial functions by PGRN

How PGRN regulates mitochondrial function specifically in males remains to be determined. Many studies have reported key differences in mitochondrial functions between males and females [16,81]. The female hormone estrogen has been shown to increase mitochondrial function and protect mitochondria under stress conditions through several different mechanisms, resulting in enhanced mitochondrial functionality in females than males under many circumstances [81]. For example, females have been shown to exhibit significantly higher mitochondrial function in peripheral blood mononuclear cells than males [67]. Females have increased resistance to brain injury, which may be related to lower mitochondrial oxidative stress and higher antioxidant defenses [3,16]. In addition, female mitochondria have been reported to metabolize more lipids than male mitochondria [81].

Several recent studies have shown a connection between PGRN and mitochondrial function. PGRN was shown to help maintain mitochondrial homeostasis through Sirt1-PGC-1α/FoxO1 mediated signaling in podocytes [91] and promote mitochondrial functions in cortical neurons in response to hyperglycemia [14]. While the mechanisms by which PGRN deficiency specifically affects male mitochondrial function remain to be fully elucidated, the protective effect of estrogen on mitochondria might render PGRN dispensable for proper

mitochondrial function in females. In this regard, it was interesting that serum estrogen levels were recently reported to increase in PGRN-deficient mice [87].

Lysosomal functions of PGRN and microglial activation

Recent studies have shown that PGRN is a lysosome resident protein [37] and is critical for proper lysosomal function [42,57]. PGRN is an evolutionarily conserved protein comprised of 7.5 granulin repeats [6]. Within the lysosome, PGRN is proteolytically cleaved into biologically active granulin peptides by cathepsins[33,93]. PGRN deficiency has been shown to result in lysosome abnormalities with aging [42,57] and lysosomal defects have been observed in PGRN-deficient microglia much earlier than neurons [24]. Thus, PGRN-deficient microglia are likely to have a defect in lysosomal degradation of myelin after the uptake of myelin debris, which might contribute to sustained microglial activation under PGRN-deficient conditions after cuprizone removal. This is supported by the upregulation of lysosomal genes in the transcriptomic analysis (Supplementary Fig. 2) and elevated levels of GPNMB, a lysosomal membrane protein, in both male and female $Grn^{-/-}$ microglia in response to cuprizone-induced demyelination and in the recovery phase (Fig. 5c, 5d). Lysosomal dysfunction caused by PGRN deficiency in microglia could cause myelination defects observed in both male and female $Grn^{-/-}$ mice and in the FTLD patients with *GRN* mutations, despite the differences in mitochondrial responses to myelin challenge in male and female $Grn^{-/-}$ microglia (Fig. 10).

In summary, our results reveal that PGRN deficiency leads to sex-dependent alterations in microglial mitochondria that influence microglial response to demyelination. Future work to dissect the mechanisms by which PGRN affects mitochondrial activities in males and lysosomal functions in microglia will help us better understand how PGRN regulates microglial functionality in the myelination process.

Data availability

The data supporting the findings of this study are included in the supplemental material. Additional data are available from the corresponding author on request. No data are deposited in databases.

Supplementary Material

Refer to Web version on PubMed Central for supplementary material.

Acknowledgments

We thank Xiaochun Wu for assistance with genotyping; Dr. Fanny Elahi, Dr. Taru Flagan and Dr. Suzee Lee (UCSF) for helpful discussions. This work is supported by NINDS/NIA (R01NS088448 & R01NS095954) to F.H.

References

1. Aldana BI (2019) Microglia-Specific Metabolic Changes in Neurodegeneration. J Mol Biol 431:1830–1842. doi:10.1016/j.jmb.2019.03.006 [PubMed: 30878483]
2. Almeida MR, Macario MC, Ramos L, Baldeiras I, Ribeiro MH, Santana I (2016) Portuguese family with the co-occurrence of frontotemporal lobar degeneration and neuronal ceroid lipofuscinosis

phenotypes due to progranulin gene mutation. Neurobiol Aging 41:200 e201–205. doi:10.1016/j.neurobiolaging.2016.02.019S0197-4580(16)00178-0 [pii]

3. Arambula SE, Reinl EL, El Demerdash N, McCarthy MM, Robertson CL (2019) Sex differences in pediatric traumatic brain injury. Exp Neurol 317:168–179. doi:10.1016/j.expneurol.2019.02.016 [PubMed: 30831070]
4. Babicki S, Arndt D, Marcu A, Liang Y, Grant JR, Maciejewski A, Wishart DS (2016) Heatmapper: web-enabled heat mapping for all. Nucleic Acids Res 44:W147–153. doi:10.1093/nar/gkw419 [PubMed: 27190236]
5. Baker M, Mackenzie IR, Pickering-Brown SM, Gass J, Rademakers R, Lindholm C, Snowden J, Adamson J, Sadovnick AD, Rollinson S, Cannon A, Dwosh E, Neary D, Melquist S, Richardson A, Dickson D, Berger Z, Eriksen J, Robinson T, Zehr C, Dickey CA, Crook R, McGowan E, Mann D, Boeve B, Feldman H, Hutton M (2006) Mutations in progranulin cause tau-negative frontotemporal dementia linked to chromosome 17. Nature 442:916–919. doi:10.1038/nature05016 [PubMed: 16862116]
6. Bateman A, Bennett HP (2009) The granulin gene family: from cancer to dementia. Bioessays 31:1245–1254. doi:10.1002/bies.200900086 [PubMed: 19795409]
7. Beel S, Moisse M, Damme M, De Muynck L, Robberecht W, Van Den Bosch L, Saftig P, Van Damme P (2017) Progranulin functions as a cathepsin D chaperone to stimulate axonal outgrowth in vivo. Hum Mol Genet 26:2850–2863. doi:10.1093/hmg/ddx1623768439 [pii] [PubMed: 28453791]
8. Burns JC, Cotleur B, Walther DM, Bajrami B, Rubino SJ, Wei R, Franchimont N, Cotman SL, Ransohoff RM, Mingueneau M (2020) Differential accumulation of storage bodies with aging defines discrete subsets of microglia in the healthy brain. Elife 9. doi:10.7554/eLife.57495
9. Cantoni C, Bollman B, Licastro D, Xie M, Mikesell R, Schmidt R, Yuede CM, Galimberti D, Olivecrona G, Klein RS, Cross AH, Otero K, Piccio L (2015) TREM2 regulates microglial cell activation in response to demyelination in vivo. Acta Neuropathol 129:429–447. doi:10.1007/s00401-015-1388-1 [PubMed: 25631124]
10. Caroppo P, Le Ber I, Camuzat A, Clot F, Naccache L, Lamari F, De Septenville A, Bertrand A, Belliard S, Hannequin D, Colliot O, Brice A (2014) Extensive white matter involvement in patients with frontotemporal lobar degeneration: think progranulin. JAMA Neurol 71:1562–1566. doi:10.1001/jamaneurol.2014.1316 [PubMed: 25317628]
11. Chausse B, Kakimoto PA, Kann O (2021) Microglia and lipids: how metabolism controls brain innate immunity. Semin Cell Dev Biol 112:137–144. doi:10.1016/j.semcdb.2020.08.001 [PubMed: 32807643]
12. Colonna M, Butovsky O (2017) Microglia Function in the Central Nervous System During Health and Neurodegeneration. Annu Rev Immunol 35:441–468. doi:10.1146/annurev-immunol-051116-052358 [PubMed: 28226226]
13. Cruts M, Gijselinck I, van der Zee J, Engelborghs S, Wils H, Pirici D, Rademakers R, Vandenberghe R, Dermaut B, Martin JJ, van Duijn C, Peeters K, Sciot R, Santens P, De Pooter T, Mattheijssens M, Van den Broeck M, Cuijt I, Vennekens K, De Deyn PP, Kumar-Singh S, Van Broeckhoven C (2006) Null mutations in progranulin cause ubiquitin-positive frontotemporal dementia linked to chromosome 17q21. Nature 442:920–924. doi:10.1038/nature05017 [PubMed: 16862115]
14. Dedert C, Mishra V, Aggarwal G, Nguyen AD, Xu F (2022) Progranulin Preserves Autophagy Flux and Mitochondrial Function in Rat Cortical Neurons Under High Glucose Stress. Front Cell Neurosci 16:874258. doi:10.3389/fncel.2022.874258 [PubMed: 35880011]
15. Deleon J, Miller BL (2018) Frontotemporal dementia. Handb Clin Neurol 148:409–430. doi:10.1016/B978-0-444-64076-5.00027-2 [PubMed: 29478591]
16. Demarest TG, McCarthy MM (2015) Sex differences in mitochondrial (dys)function: Implications for neuroprotection. J Bioenerg Biomembr 47:173–188. doi:10.1007/s10863-014-9583-7 [PubMed: 25293493]
17. Dobin A, Davis CA, Schlesinger F, Drenkow J, Zaleski C, Jha S, Batut P, Chaisson M, Gingeras TR (2013) STAR: ultrafast universal RNA-seq aligner. Bioinformatics 29:15–21. doi:10.1093/bioinformatics/bts635 [PubMed: 23104886]

18. Du H, Wong MY, Zhang T, Santos MN, Hsu C, Zhang J, Yu H, Luo W, Hu F (2021) A multifaceted role of progranulin in regulating amyloid-beta dynamics and responses. Life Sci Alliance 4. doi:10.26508/lsa.202000874

19. Feng T, Sheng RR, Sole-Domenech S, Ullah M, Zhou X, Mendoza CS, Enriquez LCM, Katz II, Paushter DH, Sullivan PM, Wu X, Maxfield FR, F Hu (2020) A role of the frontotemporal lobar degeneration risk factor TMEM106B in myelination. Brain. doi:10.1093/brain/awaa154

20. Fenoglio C, Scalabrini D, Esposito F, Comi C, Cavalla P, De Riz M, Martinelli V, Piccio LM, Venturelli E, Fumagalli G, Capra R, Collimedaglia L, Ghezzi A, Rodegher ME, Vercellino M, Leone M, Giordana MT, Bresolin N, Monaco F, Comi G, Scarpini E, Martinelli-Boneschi F, Galimberti D (2010) Progranulin gene variability increases the risk for primary progressive multiple sclerosis in males. Genes Immun 11:497–503. doi:10.1038/gene.2010.18 [PubMed: 20463744]

21. Gao X, Joselin AP, Wang L, Kar A, Ray P, Bateman A, Goate AM, Wu JY (2010) Progranulin promotes neurite outgrowth and neuronal differentiation by regulating GSK-3beta. Protein Cell 1:552–562. doi:10.1007/s13238-010-0067-1 [PubMed: 21204008]

22. Gass J, Cannon A, Mackenzie IR, Boeve B, Baker M, Adamson J, Crook R, Melquist S, Kuntz K, Petersen R, Josephs K, Pickering-Brown SM, Graff-Radford N, Uitti R, Dickson D, Wszolek Z, Gonzalez J, Beach TG, Bigio E, Johnson N, Weintraub S, Mesulam M, White CL 3rd, Woodruff B, Caselli R, Hsiung GY, Feldman H, Knopman D, Hutton M, Rademakers R (2006) Mutations in progranulin are a major cause of ubiquitin-positive frontotemporal lobar degeneration. Hum Mol Genet 15:2988–3001. doi:10.1093/hmg/ddl241 [PubMed: 16950801]

23. Gass J, Lee WC, Cook C, Finch N, Stetler C, Jansen-West K, Lewis J, Link CD, Rademakers R, Nykjaer A, Petrucelli L (2012) Progranulin regulates neuronal outgrowth independent of sortilin. Mol Neurodegener 7:33. doi:10.1186/1750-1326-7-33 [PubMed: 22781549]

24. Götzl JK, Colombo AV, Fellerer K, Reifschneider A, Werner G, Tahirovic S, Haass C, Capell A (2018) Early lysosomal maturation deficits in microglia triggers enhanced lysosomal activity in other brain cells of progranulin knockout mice. Molecular neurodegeneration 13:48. doi:10.1186/s13024-018-0281-5 [PubMed: 30180904]

25. Gudi V, Gingele S, Skripuletz T, Stangel M (2014) Glial response during cuprizone-induced de- and remyelination in the CNS: lessons learned. Front Cell Neurosci 8:73. doi:10.3389/fncel.2014.00073 [PubMed: 24659953]

26. Hammond TR, Marsh SE, Stevens B (2019) Immune Signaling in Neurodegeneration. Immunity 50:955–974. doi:10.1016/j.immuni.2019.03.016 [PubMed: 30995509]

27. Han J, Fan Y, Zhou K, Blomgren K, Harris RA (2021) Uncovering sex differences of rodent microglia. J Neuroinflammation 18:74. doi:10.1186/s12974-021-02124-z [PubMed: 33731174]

28. Han J, Zhu K, Zhou K, Hakim R, Sankavaram SR, Blomgren K, Lund H, Zhang XM, Harris RA (2020) Sex-Specific Effects of Microglia-Like Cell Engraftment during Experimental Autoimmune Encephalomyelitis. International journal of molecular sciences 21. doi:10.3390/ijms21186824

29. Hansen DV, Hanson JE, Sheng M (2018) Microglia in Alzheimer's disease. J Cell Biol 217:459–472. doi:10.1083/jcb.201709069 [PubMed: 29196460]

30. Heppner FL, Roth K, Nitsch R, Hailer NP (1998) Vitamin E induces ramification and downregulation of adhesion molecules in cultured microglial cells. Glia 22:180–188 [PubMed: 9537838]

31. Hickman S, Izzy S, Sen P, Morsett L, El Khoury J (2018) Microglia in neurodegeneration. Nat Neurosci 21:1359–1369. doi:10.1038/s41593-018-0242-x [PubMed: 30258234]

32. Hickman SE, Allison EK, El Khoury J (2008) Microglial dysfunction and defective beta-amyloid clearance pathways in aging Alzheimer's disease mice. J Neurosci 28:8354–8360. doi:10.1523/JNEUROSCI.0616-08.2008 [PubMed: 18701698]

33. Holler CJ, Taylor G, Deng Q, Kukar T (2017) Intracellular Proteolysis of Progranulin Generates Stable, Lysosomal Granulins that Are Haploinsufficient in Patients with Frontotemporal Dementia Caused by GRN Mutations. eNeuro 4. doi:10.1523/eneuro.0100-17.2017

34. Houser MC, Uriarte Huarte O, Wallings RL, Keating CE, MacPherson KP, Herrick MK, Kannarkat GT, Kelly SD, Chang J, Varvel NH, Rexach JE, Tansey MG (2022) Progranulin loss results in sex-

dependent dysregulation of the peripheral and central immune system. Frontiers in Immunology 13. doi:10.3389/fimmu.2022.1056417

35. Hoyos HC, Rinaldi M, Mendez-Huergo SP, Marder M, Rabinovich GA, Pasquini JM, Pasquini LA (2014) Galectin-3 controls the response of microglial cells to limit cuprizone-induced demyelination. Neurobiol Dis 62:441–455. doi:10.1016/j.nbd.2013.10.023 [PubMed: 24184798]
36. Hsiung GY, Fok A, Feldman HH, Rademakers R, Mackenzie IR (2011) rs5848 polymorphism and serum progranulin level. J Neurol Sci 300:28–32. doi:S0022–510X(10)00517–4 [pii]10.1016/j.jns.2010.10.009 [PubMed: 21047645]
37. Hu F, Padukkavidana T, Vaegter CB, Brady OA, Zheng Y, Mackenzie IR, Feldman HH, Nykjaer A, Strittmatter SM (2010) Sortilin-mediated endocytosis determines levels of the frontotemporal dementia protein, progranulin. Neuron 68:654–667. doi:10.1016/j.neuron.2010.09.034 [PubMed: 21092856]
38. Huang M, Modeste E, Dammer E, Merino P, Taylor G, Duong DM, Deng Q, Holler CJ, Gearing M, Dickson D, Seyfried NT, Kukar T (2020) Network analysis of the progranulin-deficient mouse brain proteome reveals pathogenic mechanisms shared in human frontotemporal dementia caused by GRN mutations. Acta Neuropathol Commun 8:163. doi:10.1186/s40478-020-01037-x [PubMed: 33028409]
39. Hyman BT, Phelps CH, Beach TG, Bigio EH, Cairns NJ, Carrillo MC, Dickson DW, Duyckaerts C, Frosch MP, Masliah E, Mirra SS, Nelson PT, Schneider JA, Thal DR, Thies B, Trojanowski JQ, Vinters HV, Montine TJ (2012) National Institute on Aging-Alzheimer's Association guidelines for the neuropathologic assessment of Alzheimer's disease. Alzheimers Dement 8:1–13. doi:10.1016/j.jalz.2011.10.007S1552-5260(11)02980-3 [PubMed: 22265587]
40. Jurga AM, Paleczna M, Kuter KZ (2020) Overview of General and Discriminating Markers of Differential Microglia Phenotypes. Front Cell Neurosci 14:198. doi:10.3389/fncel.2020.00198 [PubMed: 32848611]
41. Kamalainen A, Viswanathan J, Natunen T, Helisalmi S, Kauppinen T, Pikkarainen M, Pursiheimo JP, Alafuzoff I, Kivipelto M, Haapasalo A, Soininen H, Herukka SK, Hiltunen M (2013) GRN variant rs5848 reduces plasma and brain levels of granulin in Alzheimer's disease patients. J Alzheimers Dis 33:23–27. doi:10.3233/JAD-2012-120946 [PubMed: 22890097]
42. Kao AW, McKay A, Singh PP, Brunet A, Huang EJ (2017) Progranulin, lysosomal regulation and neurodegenerative disease. Nat Rev Neurosci 18:325–333. doi:10.1038/nrn.2017.36 [PubMed: 28435163]
43. Klein SL, Flanagan KL (2016) Sex differences in immune responses. Nat Rev Immunol 16:626–638. doi:10.1038/nri.2016.90 [PubMed: 27546235]
44. Krabbe G, Minami SS, Etchegaray JI, Taneja P, Djukic B, Davalos D, Le D, Lo I, Zhan L, Reichert MC, Sayed F, Merlini M, Ward ME, Perry DC, Lee SE, Sias A, Parkhurst CN, Gan WB, Akassoglou K, Miller BL, Farese RV Jr, Gan L (2017) Microglial NFkappaB-TNFalpha hyperactivation induces obsessive-compulsive behavior in mouse models of progranulin-deficient frontotemporal dementia. Proc Natl Acad Sci U S A 114:5029–5034. doi:10.1073/pnas.1700477114 [PubMed: 28438992]
45. Lee MJ, Chen TF, Cheng TW, Chiu MJ (2011) rs5848 Variant of Progranulin Gene Is a Risk of Alzheimer's Disease in the Taiwanese Population. Neurodegener Dis 8:216–220. doi:00032253810.1159/000322538 [PubMed: 21212639]
46. Love MI, Huber W, Anders S (2014) Moderated estimation of fold change and dispersion for RNA-seq data with DESeq2. Genome Biol 15:550. doi:10.1186/s13059-014-0550-8 [PubMed: 25516281]
47. Lynch MA (2022) Exploring Sex-Related Differences in Microglia May Be a Game-Changer in Precision Medicine. Front Aging Neurosci 14:868448. doi:10.3389/fnagi.2022.868448 [PubMed: 35431903]
48. Mackenzie IR, Neumann M (2016) Molecular neuropathology of frontotemporal dementia: insights into disease mechanisms from postmortem studies. J Neurochem 138 Suppl 1:54–70. doi:10.1111/jnc.13588 [PubMed: 27306735]
49. Mackenzie IR, Neumann M, Baborie A, Sampathu DM, Du Plessis D, Jaros E, Perry RH, Trojanowski JQ, Mann DM, Lee VM (2011) A harmonized classification system for FTLD-TDP pathology. Acta Neuropathol 122:111–113. doi:10.1007/s00401-011-0845-8 [PubMed: 21644037]

50. Marschallinger J, Iram T, Zardeneta M, Lee SE, Lehallier B, Haney MS, Pluvinage JV, Mathur V, Hahn O, Morgens DW, Kim J, Tevini J, Felder TK, Wolinski H, Bertozzi CR, Bassik MC, Aigner L, Wyss-Coray T (2020) Lipid-droplet-accumulating microglia represent a dysfunctional and proinflammatory state in the aging brain. Nat Neurosci 23:194–208. doi:10.1038/s41593-019-0566-1 [PubMed: 31959936]
51. Martens LH, Zhang J, Barmada SJ, Zhou P, Kamiya S, Sun B, Min SW, Gan L, Finkbeiner S, Huang EJ, Farese RV Jr., (2012) Progranulin deficiency promotes neuroinflammation and neuron loss following toxin-induced injury. J Clin Invest 122:3955–3959. doi:10.1172/JCI63113 [PubMed: 23041626]
52. Matsushima GK, Morell P (2001) The neurotoxicant, cuprizone, as a model to study demyelination and remyelination in the central nervous system. Brain Pathol 11:107–116. doi:10.1111/j.1750-3639.2001.tb00385.x [PubMed: 11145196]
53. Miron VE, Boyd A, Zhao JW, Yuen TJ, Ruckh JM, Shadrach JL, van Wijngaarden P, Wagers AJ, Williams A, Franklin RJM, Ffrench-Constant C (2013) M2 microglia and macrophages drive oligodendrocyte differentiation during CNS remyelination. Nature neuroscience 16:1211–1218. doi:10.1038/nn.3469 [PubMed: 23872599]
54. Nelson PT, Dickson DW, Trojanowski JQ, Jack CR, Boyle PA, Arfanakis K, Rademakers R, Alafuzoff I, Attems J, Brayne C, Coyle-Gilchrist ITS, Chui HC, Fardo DW, Flanagan ME, Halliday G, Hokkanen SRK, Hunter S, Jicha GA, Katsumata Y, Kawas CH, Keene CD, Kovacs GG, Kukull WA, Levey AI, Makkinejad N, Montine TJ, Murayama S, Murray ME, Nag S, Rissman RA, Seeley WW, Sperling RA, White CL Iii, Yu L, Schneider JA (2019) Limbic-predominant age-related TDP-43 encephalopathy (LATE): consensus working group report. Brain 142:1503–1527. doi:10.1093/brain/awz099 [PubMed: 31039256]
55. Nicholson AM, Gass J, Petrucelli L, Rademakers R (2012) Progranulin axis and recent developments in frontotemporal lobar degeneration. Alzheimers Res Ther 4:4. doi:alzrt102 [pii]10.1186/alzrt102 [PubMed: 22277331]
56. Parkhurst CN, Yang G, Ninan I, Savas JN, Yates JR 3rd, Lafaille JJ, Hempstead BL, Littman DR, Gan WB (2013) Microglia promote learning-dependent synapse formation through brain-derived neurotrophic factor. Cell 155:1596–1609. doi:10.1016/j.cell.2013.11.030 [PubMed: 24360280]
57. Paushter DH, Du H, Feng T, Hu F (2018) The lysosomal function of progranulin, a guardian against neurodegeneration. Acta Neuropathol 136:1–17. doi:10.1007/s00401-018-1861-8 [PubMed: 29744576]
58. Perry DC, Lehmann M, Yokoyama JS, Karydas A, Lee JJ, Coppola G, Grinberg LT, Geschwind D, Seeley WW, Miller BL, Rosen H, Rabinovici G (2013) Progranulin mutations as risk factors for Alzheimer disease. JAMA Neurol 70:774–778. doi:10.1001/2013.jamaneurol.3931680455 [pii] [PubMed: 23609919]
59. Poliani PL, Wang Y, Fontana E, Robinette ML, Yamanishi Y, Gilfillan S, Colonna M (2015) TREM2 sustains microglial expansion during aging and response to demyelination. J Clin Invest 125:2161–2170. doi:10.1172/JCI77983 [PubMed: 25893602]
60. Ransohoff RM, Cardona AE (2010) The myeloid cells of the central nervous system parenchyma. Nature 468:253–262. doi:10.1038/nature09615 [PubMed: 21068834]
61. Rhinn H, Abeliovich A (2017) Differential Aging Analysis in Human Cerebral Cortex Identifies Variants in TMEM106B and GRN that Regulate Aging Phenotypes. Cell Syst 4:404–415 e405. doi:10.1016/j.cels.2017.02.009 [PubMed: 28330615]
62. Roberson ED (2012) Mouse models of frontotemporal dementia. Ann Neurol 72:837–849. doi:10.1002/ana.23722 [PubMed: 23280835]
63. Salzer JL, Zalc B (2016) Myelination. Curr Biol 26:R971–R975. doi:10.1016/j.cub.2016.07.074 [PubMed: 27780071]
64. Santos EN, Fields RD (2021) Regulation of myelination by microglia. Sci Adv 7:eabk1131. doi:10.1126/sciadv.abk1131
65. Schmidt CA, Fisher-Wellman KH, Neufer PD (2021) From OCR and ECAR to energy: Perspectives on the design and interpretation of bioenergetics studies. J Biol Chem 297:101140. doi:10.1016/j.jbc.2021.101140 [PubMed: 34461088]

66. Sheng J, Su L, Xu Z, Chen G (2014) Progranulin polymorphism rs5848 is associated with increased risk of Alzheimer's disease. Gene 542:141–145. doi:10.1016/j.gene.2014.03.041S0378-1119(14)00352-7 [pii] [PubMed: 24680777]

67. Silaidos C, Pilatus U, Grewal R, Matura S, Lienerth B, Pantel J, Eckert GP (2018) Sex-associated differences in mitochondrial function in human peripheral blood mononuclear cells (PBMCs) and brain. Biol Sex Differ 9:34. doi:10.1186/s13293-018-0193-7 [PubMed: 30045765]

68. Simons M, Lyons DA (2013) Axonal selection and myelin sheath generation in the central nervous system. Current opinion in cell biology 25:512–519. doi:10.1016/j.ceb.2013.04.007 [PubMed: 23707197]

69. Skripuletz T, Lindner M, Kotsiari A, Garde N, Fokuhl J, Linsmeier F, Trebst C, Stangel M (2008) Cortical demyelination is prominent in the murine cuprizone model and is strain-dependent. Am J Pathol 172:1053–1061. doi:10.2353/ajpath.2008.070850 [PubMed: 18349131]

70. Smith KR, Damiano J, Franceschetti S, Carpenter S, Canafoglia L, Morbin M, Rossi G, Pareyson D, Mole SE, Staropoli JF, Sims KB, Lewis J, Lin WL, Dickson DW, Dahl HH, Bahlo M, Berkovic SF (2012) Strikingly different clinicopathological phenotypes determined by progranulin-mutation dosage. Am J Hum Genet 90:1102–1107. doi:10.1016/j.ajhg.2012.04.021S0002-9297(12)00254-6 [pii] [PubMed: 22608501]

71. Stepien KM, Roncaroli F, Turton N, Hendriksz CJ, Roberts M, Heaton RA, Hargreaves I (2020) Mechanisms of Mitochondrial Dysfunction in Lysosomal Storage Disorders: A Review. J Clin Med 9. doi:10.3390/jcm9082596

72. Stidworthy MF, Genoud S, Suter U, Mantei N, Franklin RJ (2003) Quantifying the early stages of remyelination following cuprizone-induced demyelination. Brain Pathol 13:329–339. doi:10.1111/j.1750-3639.2003.tb00032.x [PubMed: 12946022]

73. Subramanian A, Tamayo P, Mootha VK, Mukherjee S, Ebert BL, Gillette MA, Paulovich A, Pomeroy SL, Golub TR, Lander ES, Mesirov JP (2005) Gene set enrichment analysis: a knowledge-based approach for interpreting genome-wide expression profiles. Proc Natl Acad Sci U S A 102:15545–15550. doi:10.1073/pnas.0506580102 [PubMed: 16199517]

74. Tanaka Y, Chambers JK, Matsuwaki T, Yamanouchi K, Nishihara M (2014) Possible involvement of lysosomal dysfunction in pathological changes of the brain in aged progranulin-deficient mice. Acta Neuropathol Commun 2:78. doi:10.1186/s40478-014-0078-x [PubMed: 25022663]

75. Tanaka Y, Suzuki G, Matsuwaki T, Hosokawa M, Serrano G, Beach TG, Yamanouchi K, Hasegawa M, Nishihara M (2017) Progranulin regulates lysosomal function and biogenesis through acidification of lysosomes. Hum Mol Genet 26:969–988. doi:10.1093/hmg/ddx011 [PubMed: 28073925]

76. Ugidos IF, Pistono C, Korhonen P, Gomez-Budia M, Sitnikova V, Klecki P, Stanova I, Jolkkonen J, Malm T (2022) Sex Differences in Poststroke Inflammation: a Focus on Microglia Across the Lifespan. Stroke 53:1500–1509. doi:10.1161/STROKEAHA.122.039138 [PubMed: 35468000]

77. Van Damme P, Van Hoecke A, Lambrechts D, Vanacker P, Bogaert E, van Swieten J, Carmeliet P, Van Den Bosch L, Robberecht W (2008) Progranulin functions as a neurotrophic factor to regulate neurite outgrowth and enhance neuronal survival. J Cell Biol 181:37–41. doi:10.1083/jcb.200712039 [PubMed: 18378771]

78. Van Deerlin VM, Sleiman PM, Martinez-Lage M, Chen-Plotkin A, Wang LS, Graff-Radford NR, Dickson DW, Rademakers R, Boeve BF, Grossman M, Arnold SE, Mann DM, Pickering-Brown SM, Seelaar H, Heutink P, van Swieten JC, Murrell JR, Ghetti B, Spina S, Grafman J, Hodges J, Spillantini MG, Gilman S, Lieberman AP, Kaye JA, Woltjer RL, Bigio EH, Mesulam M, Al-Sarraj S, Troakes C, Rosenberg RN, White CL 3rd, Ferrer I, Llado A, Neumann M, Kretzschmar HA, Hulette CM, Welsh-Bohmer KA, Miller BL, Alzualde A, Lopez de Munain A, McKee AC, Gearing M, Levey AI, Lah JJ, Hardy J, Rohrer JD, Lashley T, Mackenzie IR, Feldman HH, Hamilton RL, Dekosky ST, van der Zee J, Kumar-Singh S, Van Broeckhoven C, Mayeux R, Vonsattel JP, Troncoso JC, Kril JJ, Kwok JB, Halliday GM, Bird TD, Ince PG, Shaw PJ, Cairns NJ, Morris JC, McLean CA, DeCarli C, Ellis WG, Freeman SH, Frosch MP, Growdon JH, Perl DP, Sano M, Bennett DA, Schneider JA, Beach TG, Reiman EM, Woodruff BK, Cummings J, Vinters HV, Miller CA, Chui HC, Alafuzoff I, Hartikainen P, Seilhean D, Galasko D, Masliah E, Cotman CW, Tunon MT, Martinez MC, Munoz DG, Carroll SL, Marson D, Riederer PF, Bogdanovic N, Schellenberg GD, Hakonarson H, Trojanowski JQ, Lee VM (2010) Common variants at 7p21

are associated with frontotemporal lobar degeneration with TDP-43 inclusions. Nat Genet 42:234–239. doi:10.1038/ng.536 [PubMed: 20154673]

79. van der Lienden MJC, Gaspar P, Boot R, Aerts J, van Eijk M (2018) Glycoprotein Non-Metastatic Protein B: An Emerging Biomarker for Lysosomal Dysfunction in Macrophages. International journal of molecular sciences 20. doi:10.3390/ijms20010066
80. Varet H, Brillet-Gueguen L, Coppee JY, Dillies MA (2016) SARTools: A DESeq2- and EdgeR-Based R Pipeline for Comprehensive Differential Analysis of RNA-Seq Data. PLoS One 11:e0157022. doi:10.1371/journal.pone.0157022 [PubMed: 27280887]
81. Ventura-Clapier R, Moulin M, Piquereau J, Lemaire C, Mericskay M, Veksler V, Garnier A (2017) Mitochondria: a central target for sex differences in pathologies. Clin Sci (Lond) 131:803–822. doi:10.1042/CS20160485 [PubMed: 28424375]
82. Vercellino M, Fenoglio C, Galimberti D, Mattioda A, Chiavazza C, Binello E, Pinessi L, Giobbe D, Scarpini E, Cavalla P (2016) Progranulin genetic polymorphisms influence progression of disability and relapse recovery in multiple sclerosis. Mult Scler 22:1007–1012. doi:10.1177/1352458515610646 [PubMed: 26447062]
83. Vercellino M, Grifoni S, Romagnolo A, Masera S, Mattioda A, Trebini C, Chiavazza C, Caligiana L, Capello E, Mancardi GL, Giobbe D, Mutani R, Giordana MT, Cavalla P (2011) Progranulin expression in brain tissue and cerebrospinal fluid levels in multiple sclerosis. Mult Scler 17:1194–1201. doi:10.1177/1352458511406164 [PubMed: 21613335]
84. Woollacott IOC, Bocchetta M, Sudre CH, Ridha BH, Strand C, Courtney R, Ourselin S, Cardoso MJ, Warren JD, Rossor MN, Revesz T, Fox NC, Holton JL, Lashley T, Rohrer JD (2018) Pathological correlates of white matter hyperintensities in a case of progranulin mutation associated frontotemporal dementia. Neurocase 24:166–174. doi:10.1080/13554794.2018.1506039 [PubMed: 30112957]
85. Wu Y, Shao W, Todd TW, Tong J, Yue M, Koga S, Castanedes-Casey M, Librero AL, Lee CW, Mackenzie IR, Dickson DW, Zhang YJ, Petrucelli L, Prudencio M (2021) Microglial lysosome dysfunction contributes to white matter pathology and TDP-43 proteinopathy in GRN-associated FTD. Cell Rep 36:109581. doi:10.1016/j.celrep.2021.109581 [PubMed: 34433069]
86. Xu HM, Tan L, Wan Y, Tan MS, Zhang W, Zheng ZJ, Kong LL, Wang ZX, Jiang T, Tan L, Yu JT (2017) PGRN Is Associated with Late-Onset Alzheimer's Disease: a Case-Control Replication Study and Meta-analysis. Mol Neurobiol 54:1187–1195. doi:10.1007/s12035-016-9698-4 [PubMed: 26820675]
87. Yang Y, Feng N, Liang L, Jiang R, Pan Y, Geng N, Fan M, Li X, Guo F (2022) Progranulin, a moderator of estrogen/estrogen receptor alpha binding, regulates bone homeostasis through PERK/p-eIF2 signaling pathway. J Mol Med (Berl) 100:1191–1207. doi:10.1007/s00109-022-02233-z [PubMed: 35838759]
88. Yin F, Banerjee R, Thomas B, Zhou P, Qian L, Jia T, Ma X, Ma Y, Iadecola C, Beal MF, Nathan C, Ding A (2010) Exaggerated inflammation, impaired host defense, and neuropathology in progranulin-deficient mice. J Exp Med 207:117–128. doi:jem.20091568 [pii]10.1084/jem.20091568 [PubMed: 20026663]
89. Zerbino DR, Achuthan P, Akanni W, Amode MR, Barrell D, Bhai J, Billis K, Cummins C, Gall A, Giron CG, Gil L, Gordon L, Haggerty L, Haskell E, Hourlier T, Izuogu OG, Janacek SH, Juettemann T, To JK, Laird MR, Lavidas I, Liu Z, Loveland JE, Maurel T, McLaren W, Moore B, Mudge J, Murphy DN, Newman V, Nuhn M, Ogeh D, Ong CK, Parker A, Patricio M, Riat HS, Schuilenburg H, Sheppard D, Sparrow H, Taylor K, Thormann A, Vullo A, Walts B, Zadissa A, Frankish A, Hunt SE, Kostadima M, Langridge N, Martin FJ, Muffato M, Perry E, Ruffier M, Staines DM, Trevanion SJ, Aken BL, Cunningham F, Yates A, Flicek P (2018) Ensembl 2018. Nucleic Acids Res 46:D754–D761. doi:10.1093/nar/gkx1098 [PubMed: 29155950]
90. Zhang T, Du H, Santos MN, Wu X, Pagan MD, Trigiani LJ, Nishimura N, Reinheckel T, Hu F (2022) Differential regulation of progranulin derived granulin peptides. Mol Neurodegener 17:15. doi:10.1186/s13024-021-00513-9 [PubMed: 35120524]
91. Zhou D, Zhou M, Wang Z, Fu Y, Jia M, Wang X, Liu M, Zhang Y, Sun Y, Lu Y, Tang W, Yi F (2019) PGRN acts as a novel regulator of mitochondrial homeostasis by facilitating mitophagy and mitochondrial biogenesis to prevent podocyte injury in diabetic nephropathy. Cell Death Dis 10:524. doi:10.1038/s41419-019-1754-3 [PubMed: 31285425]

92. Zhou X, Nicholson AM, Ren Y, Brooks M, Jiang P, Zuberi A, Phuoc HN, Perkerson RB, Matchett B, Parsons TM, Finch NA, Lin W, Qiao W, Castanedes-Casey M, Phillips V, Librero AL, Asmann Y, Bu G, Murray ME, Lutz C, Dickson DW, Rademakers R (2020) Loss of TMEM106B leads to myelination deficits: implications for frontotemporal dementia treatment strategies. Brain 143:1905–1919. doi:10.1093/brain/awaa141 [PubMed: 32504082]

93. Zhou X, Paushter DH, Feng T, Sun L, Reinheckel T, Hu F (2017) Lysosomal processing of progranulin. Mol Neurodegener 12:62. doi:10.1186/s13024-017-0205-9 [PubMed: 28835281]

94. Zhou X, Sun L, Bracko O, Choi JW, Jia Y, Nana AL, Brady OA, Hernandez JCC, Nishimura N, Seeley WW, Hu F (2017) Impaired prosaposin lysosomal trafficking in frontotemporal lobar degeneration due to progranulin mutations. Nat Commun 8:15277. doi:10.1038/ncomms15277 [PubMed: 28541286]

95. Zirngibl M, Assinck P, Sizov A, Caprariello AV, Plemel JR (2022) Oligodendrocyte death and myelin loss in the cuprizone model: an updated overview of the intrinsic and extrinsic causes of cuprizone demyelination. Mol Neurodegener 17:34. doi:10.1186/s13024-022-00538-8 [PubMed: 35526004]

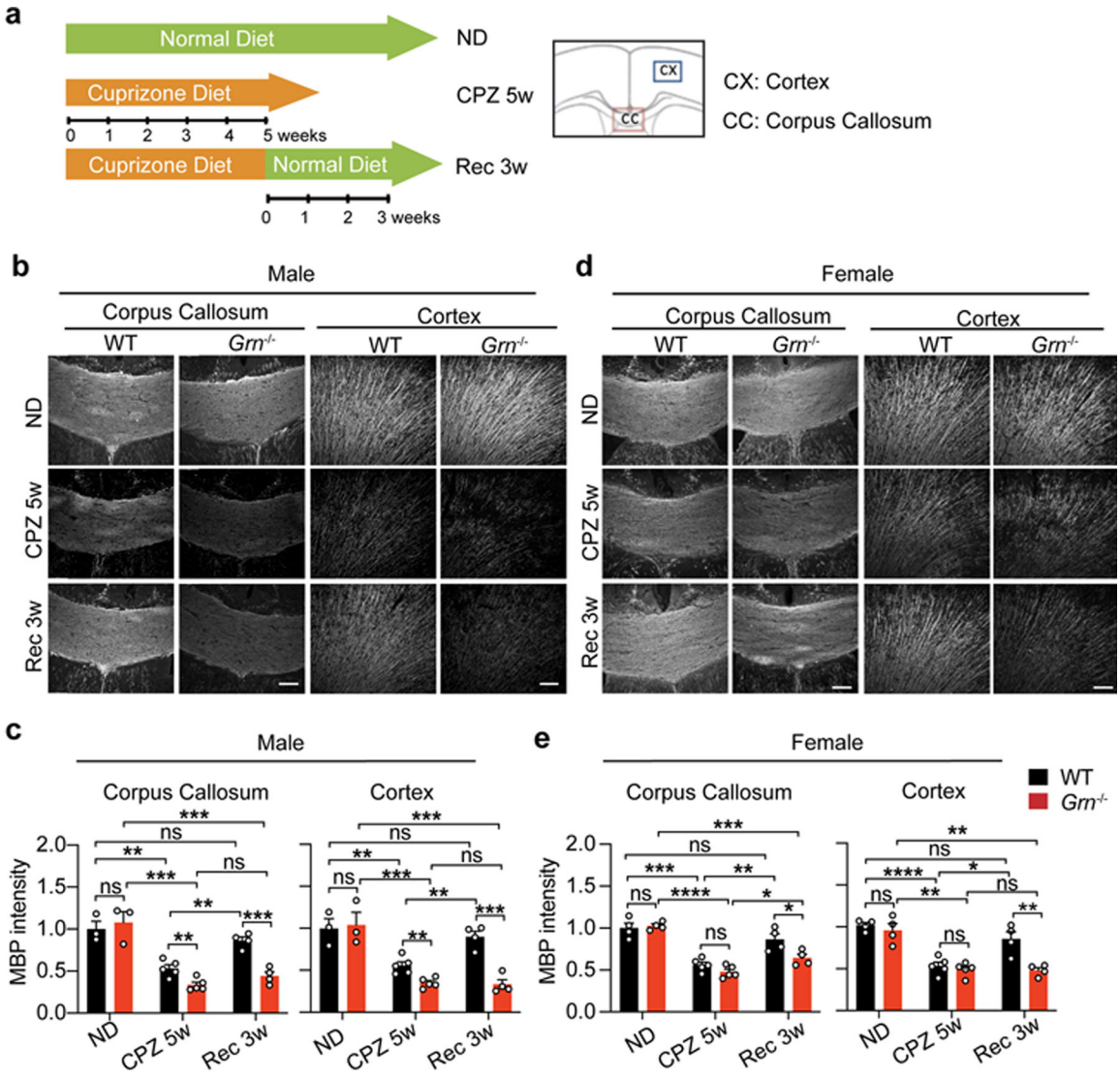

Fig. 1. PGRN deficiency results in myelination deficits in a sex-dependent manner.

a Experimental design for the cuprizone-induced demyelination mouse model. 10 weeks old male and female *Grn*$^{-/-}$ mice and littermate wildtype (WT) mice were fed with normal diet (ND), or cuprizone-containing diet (CPZ 5w) for 5 weeks. Another group of mice was fed with a normal diet for 3 weeks after 5 weeks of cuprizone treatment (Rec 3w). Coronal brain sections were stained with MBP antibody. **b-e** Representative images from the corpus callosum region and frontal cortex were shown for experiments described in (**a**). Scale bar = 100 μm. MBP intensity was quantified in (**c**) and (**e**) from male and female mice, respectively. Data represent the mean ± SEM. Statistical significance was analyzed by unpaired two-tailed Student's t-test (n = 3–5 mice per group). ns, not significant, *p < 0.05; **p < 0.01; ***p < 0.001; ****p < 0.0001.

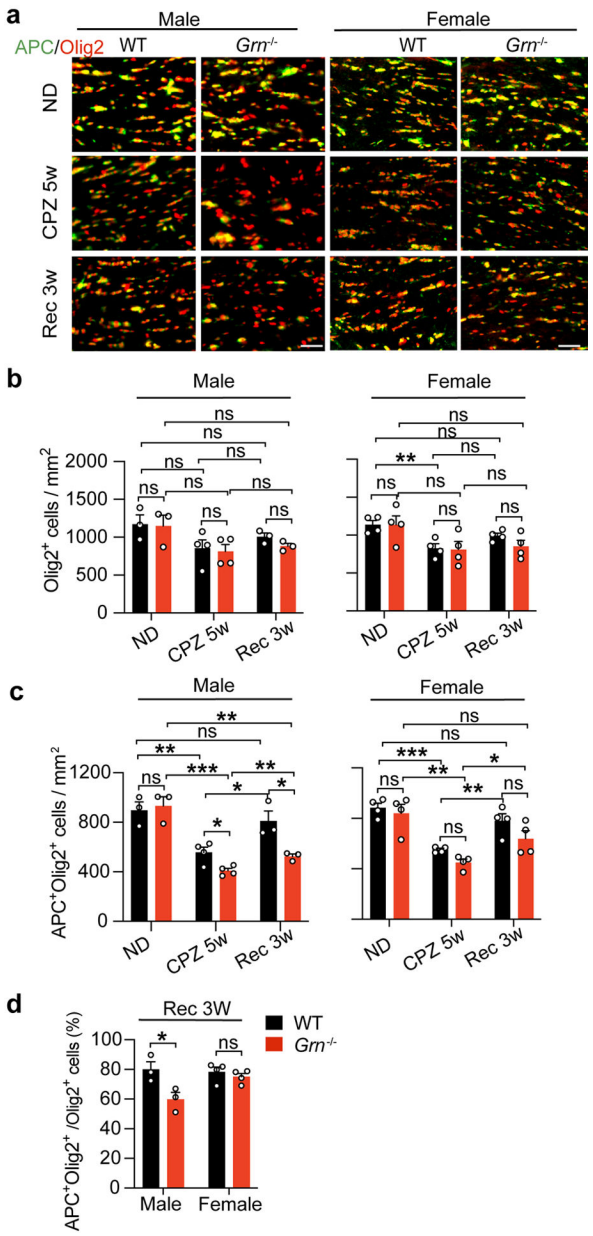

Fig. 2. PGRN deficiency results in the loss of mature oligodendrocytes in response to cuprizone and oligodendrocyte differentiation defects during recovery in male mice.

a-c Brain sections were stained with antibodies against APC and OLIG2. Representative images from the corpus callosum region were shown in (**a**). Scale bar = 100 μm. Total numbers of all oligodendrocytes (OLs) (OLIG2+) and mature oligodendrocytes (APC+/OLIG2+) at different time points were quantified in (**b**) and (**c**), respectively. Data represent the mean ± SEM. Statistical significance was analyzed by unpaired two-tailed Student's t-test (n = 3–4 mice per group). ns, not significant, *, $p < 0.05$; **, $p<0.01$,***$p < 0.001$.

d The ratio of mature OLs (APC+/OLIG2+) and total OLs (OLIG2+) at Rec3w time point was quantified. Data were analyzed by unpaired two-tailed Student's t-test (n = 3–4 mice per group). ns, not significant, *$p < 0.05$.

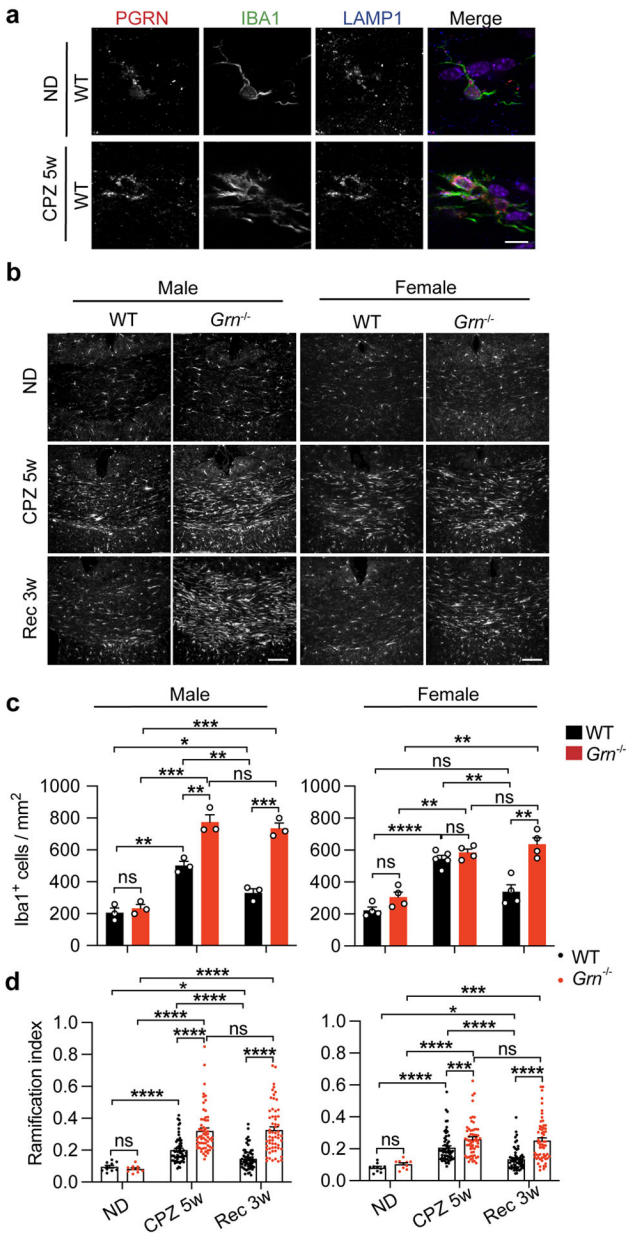

Fig. 3. PGRN deficiency leads to more pronounced microgliosis in male mice in response to demyelination.

a Brain sections from WT mice fed with ND or cuprizone-containing chow for 5 weeks (CPZ 5w) were stained with antibodies against PGRN, IBA1, and LAMP1. Representative images from the corpus callosum region were shown. Scale bar = 10 μm. **b-c** WT and *Grn*$^{-/-}$ male and female mice were fed with normal chow (ND), or cuprizone-containing chow for 3 weeks (CPZ 3w) or 5 weeks (CPZ 5w). Another group of mice was fed with normal chow for 3 weeks after 5 weeks of cuprizone treatment (Rec 3w). Brain sections were stained with IBA1 antibody. Representative images from the corpus callosum region were shown (**b**). Scale bar = 100 μm. The numbers of IBA1+ microglia in the corpus callosum region were quantified and normalized to WT (**c**). Data represent the mean ± SEM. Statistical significance was analyzed by unpaired two-tailed Student's t-test (n = 3–5 mice

per group). ns, not significant; *p < 0.05, **p < 0.01, ***p < 0.001; ****p < 0.0001. **d** A ramification index [RI = 4**π** × cell area/ (cell perimeter)^2] that describes microglial cell shape was calculated for WT and *Grn*$^{-/-}$ microglia under different conditions. 10 microglia were analyzed for mice fed with a normal diet. A total of 60 cells from 3 to 5 independent mice were analyzed for each CPZ treated and recovery group. Data represent the mean ± SEM. Statistical significance was analyzed by unpaired two-tailed Student's t-test (n = 10–60 microglia per group). ns, not significant; *p < 0.05, **p < 0.01, ***p < 0.001; ****p < 0.0001.

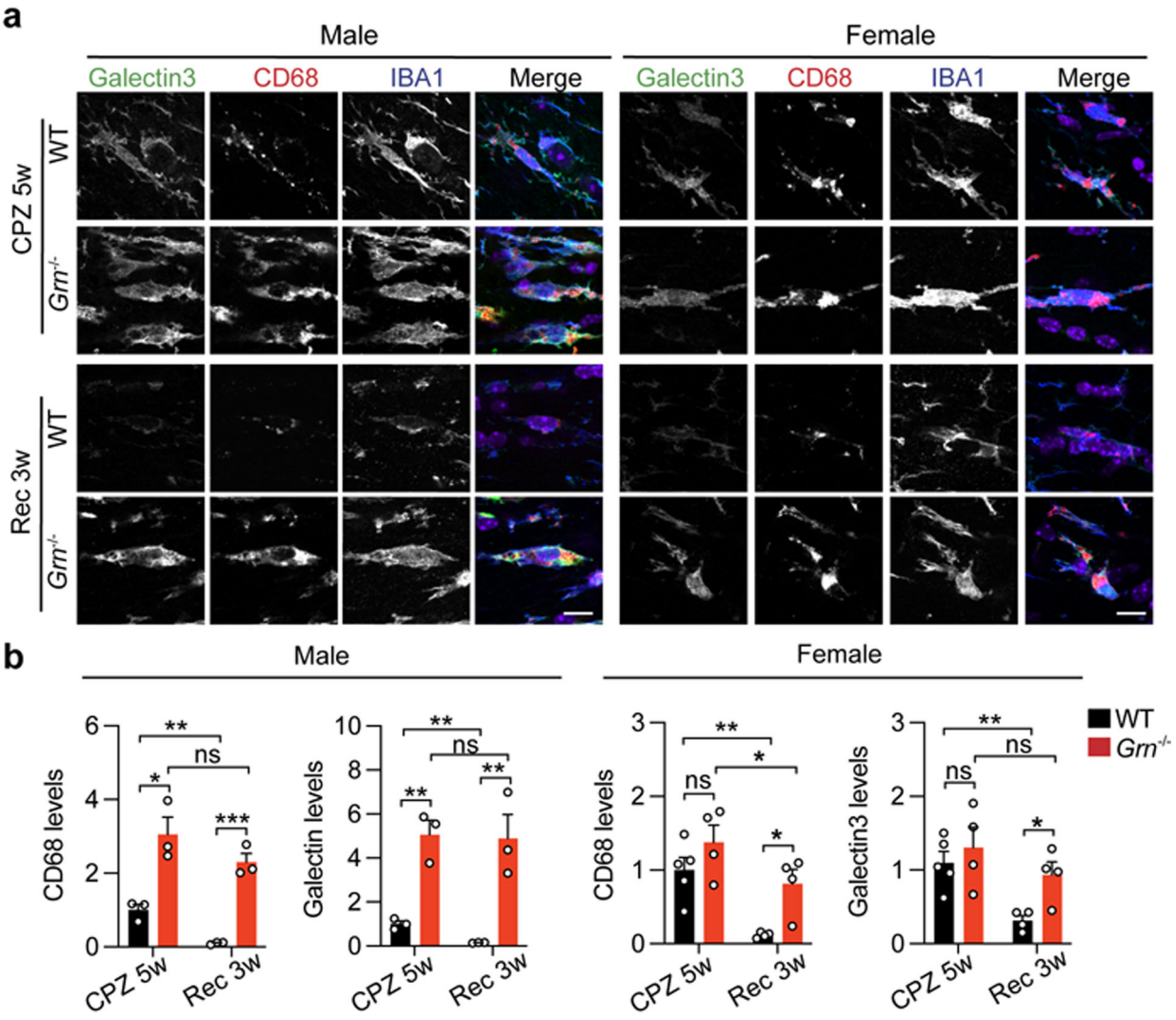

Fig. 4. PGRN deficiency leads to increased protein levels of CD68 and Galectin3 in microglia in male but not female mice in response to demyelination.

a-b WT and *Grn*$^{-/-}$ mice were fed with cuprizone-containing chow (CPZ 5w) for 5 weeks or 3 weeks after cuprizone removal (Rec 3w). Brain sections were stained with Galectin-3, CD68, and IBA1 antibodies. Representative images in the corpus callosum region were shown (**a**). Scale bar = 10 μm. CD68 and Galectin-3 levels in microglia were quantified (**b**). Data represent the mean ± SEM. Statistical significance was analyzed by unpaired two-tailed Student's t-test (n = 3–5 mice per group). ns, not significant, *p < 0.05, **p < 0.01.

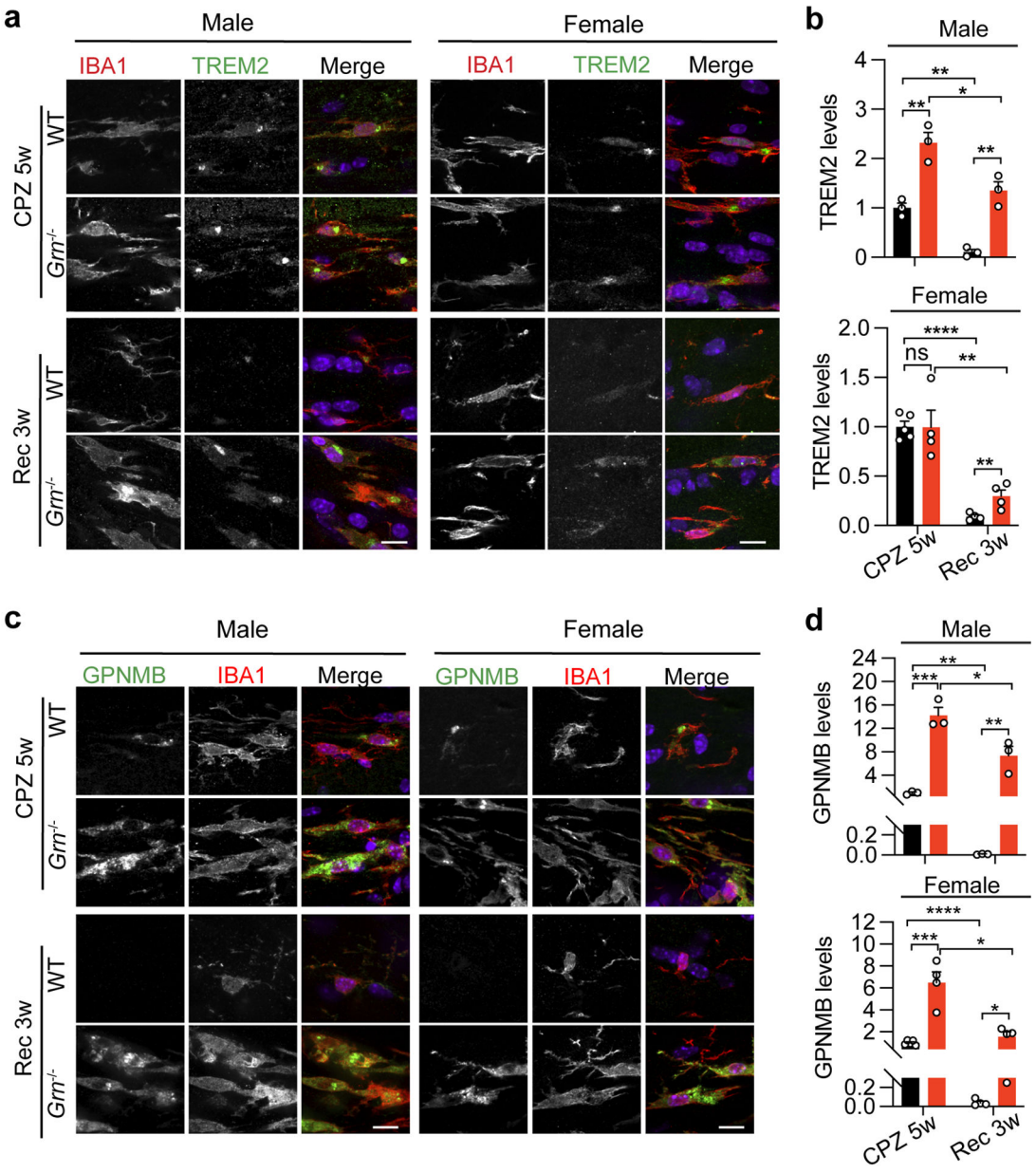

Fig. 5. PGRN deficiency leads to increased protein levels of TREM2 and GPNMB in response to demyelination.

a-d WT and *Grn*$^{-/-}$ mice were fed with cuprizone-containing chow (CPZ 5w) for 5 weeks or 3 weeks after cuprizone removal (Rec 3w). Brain sections were stained with TREM2 and IBA1 antibodies (**a**) or GPNMB and IBA1 antibodies (**c**). Representative images in the corpus callosum region were shown (**a,c**). Scale bar = 10 μm. TREM2 and GPNMB levels in microglia were quantified (b,d). Data represent the mean ± SEM. Statistical significance was analyzed by unpaired two-tailed Student's t-test (n = 3–5 mice per group). ns, not significant, *p < 0.05, **p < 0.01, ***p < 0.001, ****p < 0.0001.

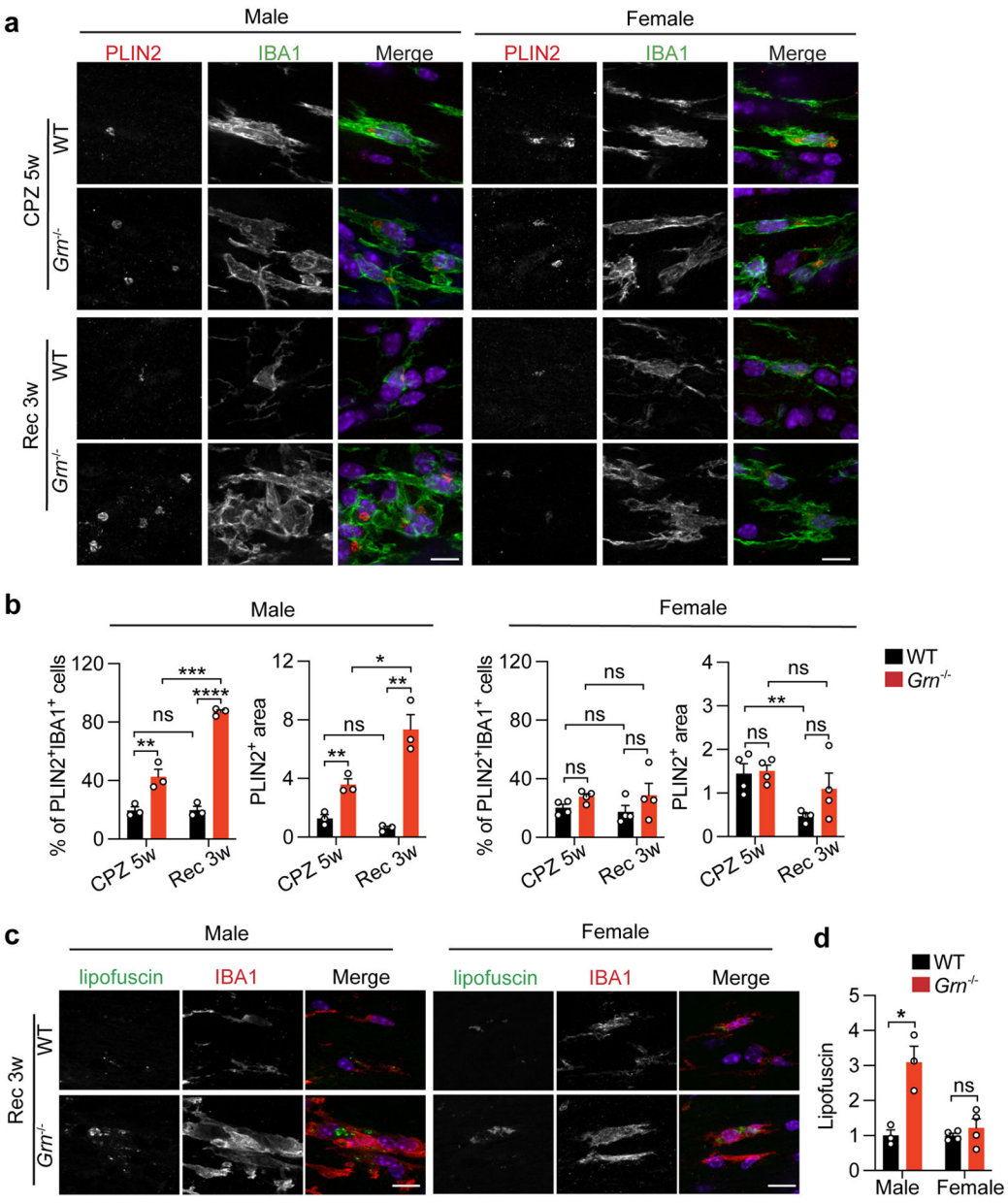

Fig. 6. PGRN deficiency leads to increased lipid droplet formation and lipofuscin accumulation in microglia in male but not female mice.

a-b Brain sections from both male and female WT and *Grn*$^{-/-}$ mice at CPZ 5w or Rec 3w were stained with Perilipin2 (PLIN2) and IBA1 antibodies. Representative images in the corpus callosum region were shown (**a**). Scale bar = 10 μm. The percentage of PLIN2+IBA1+ microglia to total microglia and the area of PLIN2+ signals in microglia were quantified, respectively (**b**). Data represent the mean ± SEM. Statistical significance was analyzed by unpaired two-tailed Student's t-test (n = 3–4 mice per group). ns, not significant, *p < 0.05, **p < 0.01, ***p < 0.001, ****p < 0.0001. **c-d** Brain sections from male WT and *Grn*$^{-/-}$ mice at Rec3w were stained with IBA1 antibody. Autofluorescent signals were imaged in the green channel. Representative images in the corpus callosum region were shown (**c**). Scale bar = 10 μm. The autofluorescent intensity in microglia was

quantified (**d**). Data represent the mean ± SEM. Statistical significance was analyzed by unpaired two-tailed Student's t-test (n = 3–4 mice per group). *p < 0.05.

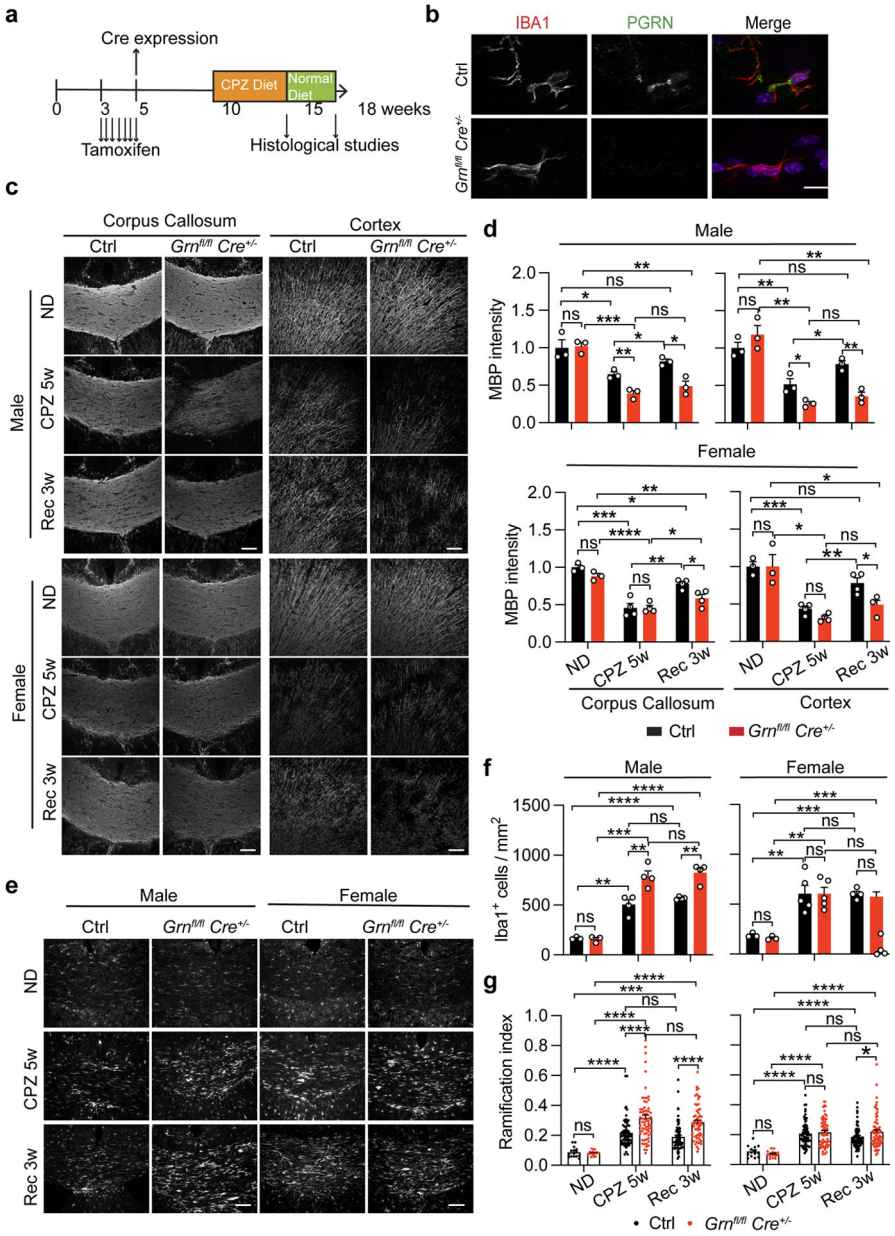

Fig. 7. Microglia-specific ablation of PGRN leads to myelination deficits and exacerbated microglia activation in male mice.

a A diagram to show the experimental design: 3-week-old *Cx3cr1*$^{+/CreER}$ *Grn*$^{flox/flox}$ mice were fed with tamoxifen to specifically delete PGRN in microglia. *Cx3cr1*$^{+/CreER}$ mice were used as controls. At 10 weeks of age, these mice were fed with a normal diet (ND) or cuprizone-containing diet (CPZ 5w) for 5 weeks. For another group of mice, cuprizone was removed for 3 weeks to allow recovery (Rec 3w). **b** 10 weeks after Tamoxifen treatment, *Cx3cr1*$^{+/CreER}$ mice (ctrl) and *Cx3cr1*$^{+/CreER}$ *Grn* $^{flox/flox}$ mice (Grn$^{fl/fl}$) were perfused and brain sections were stained with antibodies against PGRN and IBA1. Representative images from the corpus callosum region were shown. Scale bar = 10 μm. **c,d** Coronal brain sections from male and female *Cx3cr1*$^{+/CreER}$ mice (ctrl) and *Cx3cr1*$^{+/CreER}$ *Grn* $^{flox/flox}$ mice (Grn$^{fl/fl}$) at different time points were stained with MBP antibodies. Representative images

from the corpus callosum region and frontal cortex were shown. Scale bar = 100 μm. MBP intensity was quantified in (**d**). **e-f** Brain sections were stained with anti-IBA1 antibodies. Representative images from the corpus callosum region were shown. Scale bar = 100 μm. The number of IBA1-positive cells was quantified and normalized to control mice. Data represent the mean ± SEM. Statistical significance was analyzed by unpaired two-tailed Student's t-test (n = 3–5 mice per group). ns, not significant, *p < 0.05; **p < 0.01; ***p < 0.001; ****p < 0.0001. **g** A ramification index [RI = 4**π** × cell area/ (cell perimeter)^2] that describes microglial cell shape was calculated for microglia under the different conditions as indicated. 15 microglia were analyzed for mice fed with a normal diet. A total of 60 to 70 cells/ group from 3–5 independent mice/group were analyzed for each CPZ treated and recovery group. Data represent the mean ± SEM. Statistical significance was analyzed by unpaired two-tailed Student's t-test (n = 15–70 microglia per group). ns, not significant; *p < 0.05, **p < 0.01, ***p < 0.001; ****p < 0.0001.

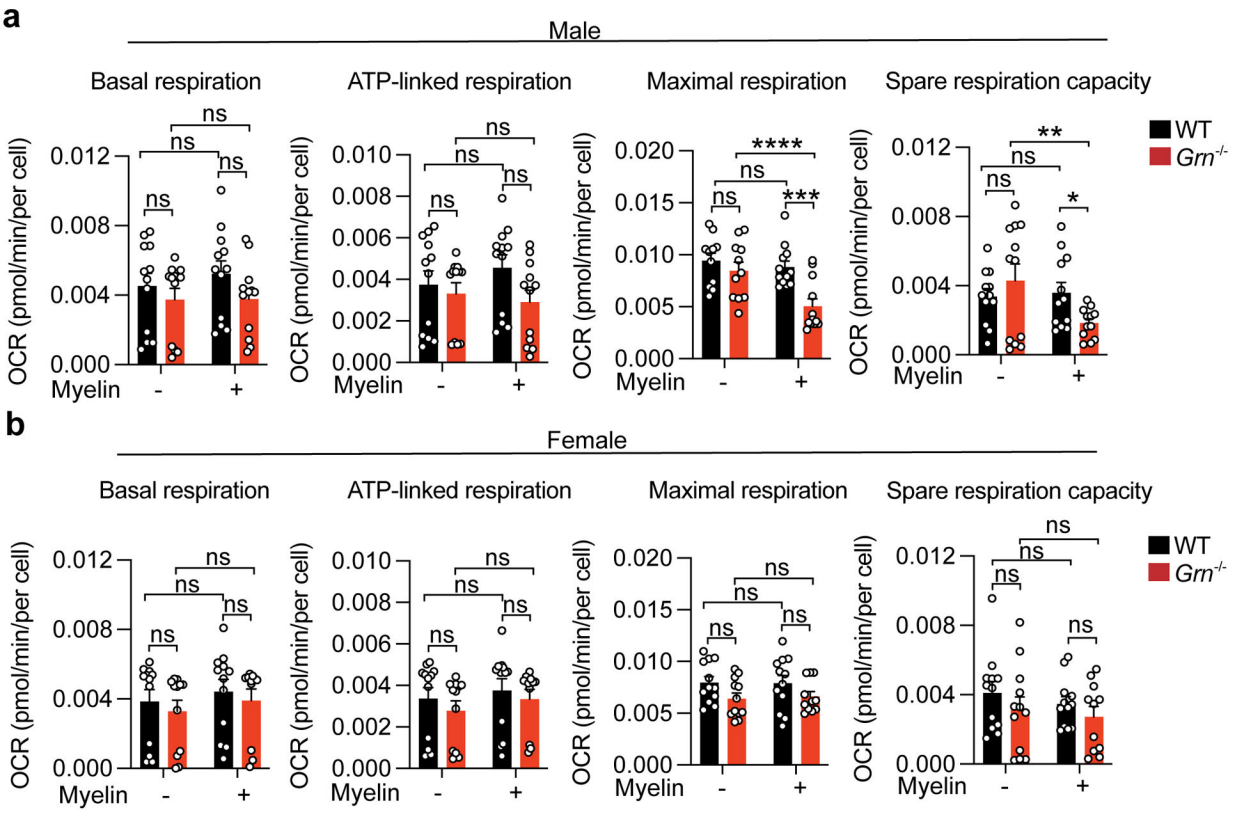

Fig. 8. PGRN deficiency leads to mitochondrial dysfunction in male microglia in response to myelin challenge.

a-b Male and female WT and *Grn*$^{-/-}$ primary microglia were fed with or without myelin for 24h and then subjected to a mitochondria stress test using the Seahorse XF96 analyzer. Oxygen consumption rates (OCR) were measured with no drug treatment (basal conditions) and with the sequential treatment of 1 μM oligomycin, 2 μM FCCP, and 0.5 μM rotenone plus antimycin A (Rote/AA). Basal respiration, ATP-linked respiration, maximal respiration, and spare respiratory capacity were calculated. Data represent the mean ± SEM. Statistical significance was analyzed by two-way ANOVA (n = 11–12). ns, not significant. *p < 0.05, **p < 0.01, ***p < 0.001, ****p < 0.0001.

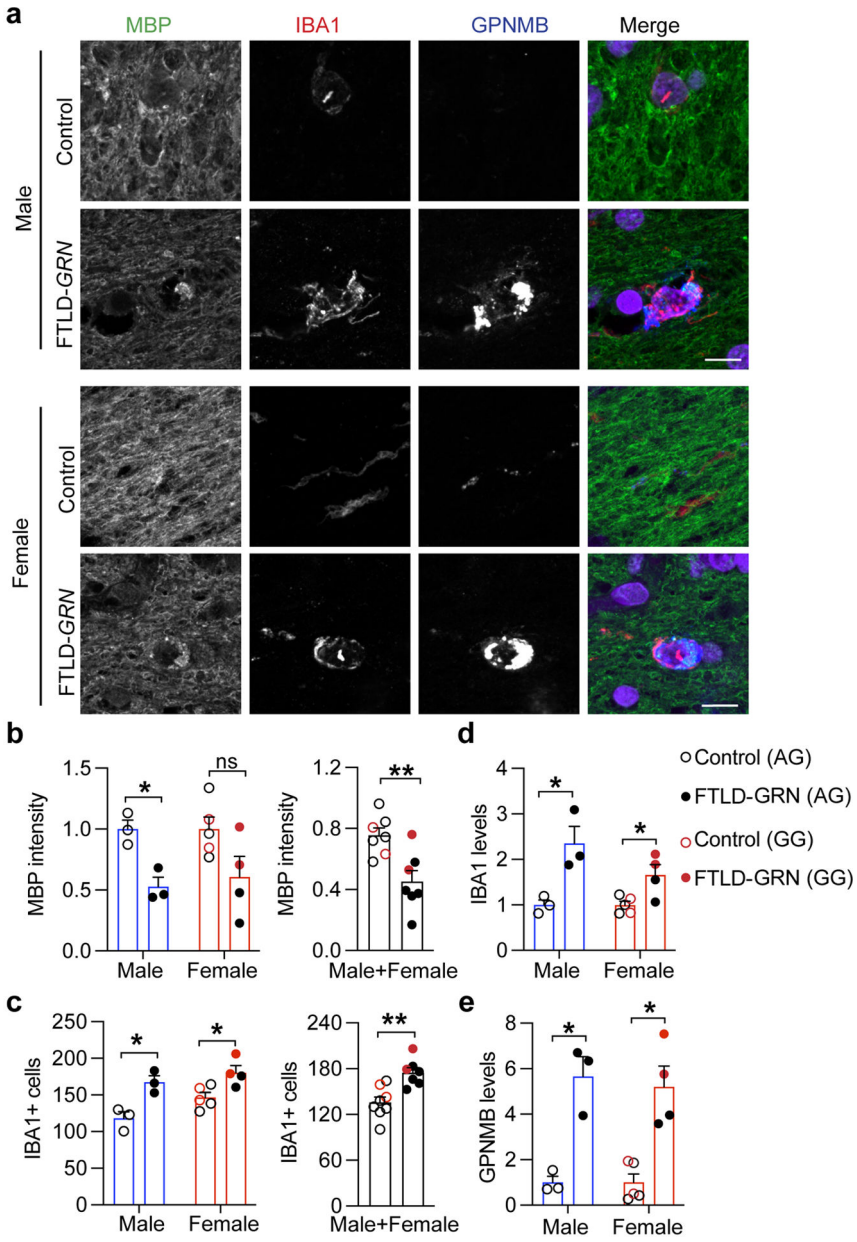

Fig. 9. Myelin loss and microglia activation in the white matter of FTLD-*GRN* patients.

a-e Corpus callosum sections of postmortem human brain tissues from healthy control subjects and patients with FTLD-TDP and carrying a *GRN* mutation (Table 1) were stained with MBP, IBA1, and GPNMB antibodies. Representative confocal images from males and females were shown (**a**). Scale bar = 10 μm. Five to ten 20X images were taken from each section for quantification. Total MBP intensities and the number of IBA1 positive microglia per image were quantified in (**b**) and (**c**), respectively. Total IBA1 levels and GPNMB levels in microglia were quantified in (**d,e**). AG and GG indicates different *TMEM106B* alleles. Data represent the mean ± SEM. Statistical significance was analyzed by unpaired two-tailed Student's t-test (n = 3 males and 4–5 females for each group). ns, not significant. *p < 0.05, **p < 0.01.

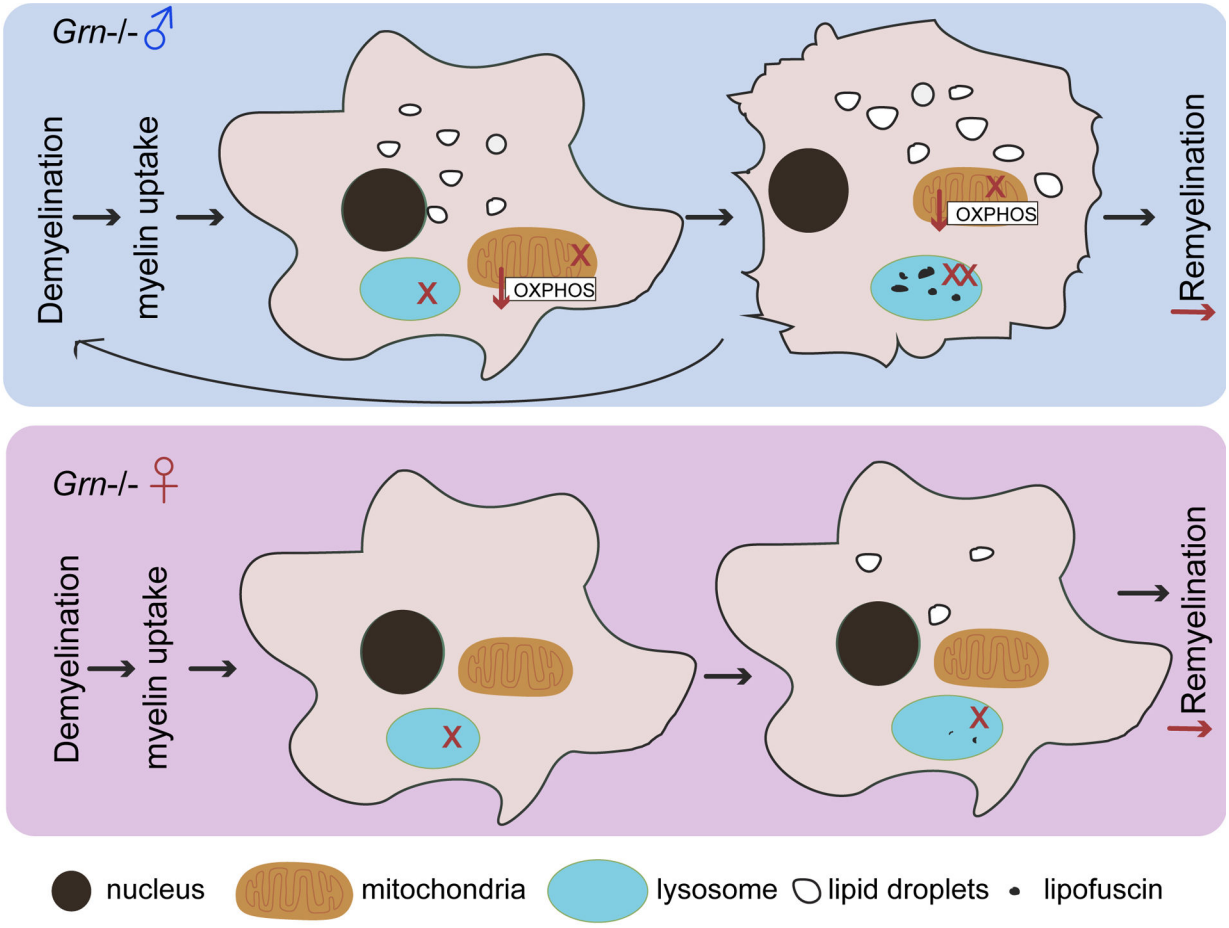

Fig. 10. A model for sex-dependent functions of PGRN in microglia to regulate myelination.

In response to demyelination, the uptake of myelin leads to mitochondrial dysfunction in male but not female *Grn*$^{-/-}$ microglia, resulting in increased lipid droplet accumulation and exacerbated microglial activation as well as lipofuscin accumulation. PGRN deficiency results in lysosomal defects in both males and females, which leads to prolonged microglial activation after cuprizone removal and a defect in re-myelination during the recovery phase. "X" indicates dysfunction in mitochondria or lysosomes.

Table 1:

List of postmortem human patient samples used in the study

Case P#	Age at death	Sex	Clinical	Primary Neuropathological Diagnosis	Other Contributing Diagnosis	GRN mutation	TMEM106B genotype	AD Thal Phase	AD Braak Stage	AD CERAD Neuritic Plaque Score	AD neuropathologic change	Lewy Body Disease Stage
Control1	78	F	Control	None		Negative	AG	1	4	0	Low	0
Control2	76	M	Control	None		Negative	AG	1	2	1	Low	0
Control3	94	M	Control	VBI	FTLD-tau, unclassifiable	Negative	AG	2	1	3	Low	Brainstem predominant
Control4	91	M	Control	None		Negative	AG	2	2	1	Low	0
Control5	92	F	Control	None	AGD	Negative	AG	0	2	0	Not ADNC	0
Control6	84	F	Control	None		Negative	AG	2	2	1	Low	0
Control7	86	F	Control	None	Cerebrovascular disease, AGD	Negative	GG	1	2	2	Low	0
Control8	86	F	Control	None		Negative	GG	2	3	0	Low	0
FTLD1	73	F	nfvPPA, CBS	FTLD-TDP-A		splicing(c.264+2T>C)	GG	0	2	0	Not ADNC	0
FTLD2	64	F	CBS	FTLD-TDP-A		NM_002087.2:c.708+1G>A	GG	2	1	0	Low	0
FTLD3	70	F	PPA, unspecified	FTLD-TDP-A	VBI	c.C1477T;p.R493X	AG	1	1	0	Low	0
FTLD4	56	F	bvFTD	FTLD-TDP-A		Q406X	AG	2	1	0	Low	0
FTLD5	74	M	nfvPPA	FTLD-TDP-A		c.1145delC	AG	4	5	2	High	0
FTLD6	64	M	bvFTD	FTLD-TDP-A		c.709_835delAla237fs	AG	0	2	0	Not ADNC	0
FTLD7	72	M	AD	FTLD-TDP-A		p.I422EfsX72	AG	5	6	3	High	Amygdala-predominant

AD, Alzheimer's disease; AGD, Argyrophilic grain disease; bvFTD, behavioral variant frontotemporal dementia; CBS, Corticobasal syndrome; FTLD-TDP-A, Frontotemporal lobar degeneration with TDP-43 inclusions, type A; nfvPPA, nonfluent variant primary progressive aphasia; PPA, primary progressive aphasia; VBI, vascular brain injury.